A PANEL FINITE ELEMENT WITH DISTORTIONAL MODES FOR THE
ANALYSIS OF OPEN SECTION THIN WALLED BEAMS

A THESIS SUBMITTED TO
THE GRADUATE SCHOOL OF NATURAL AND APPLIED SCIENCES
OF
MIDDLE EAST TECHNICAL UNIVERSITY

BY

SUAT ONTAÇ

IN PARTIAL FULFILLMENT OF THE REQUIREMENTS
FOR
THE DEGREE OF DOCTOR OF PHILOSOPHY
IN
MECHANICAL ENGINEERING

FEBRUARY 2023

Approval of the thesis:

THESIS TITLE

submitted by **SUAT ONTAÇ** in partial fulfillment of the requirements for the degree
of **Doctor of Philosophy** in **Mechanical Engineering, Middle East Technical
University** by,

Prof. Dr. Halil Kalıpçılar
Dean, Graduate School of **Natural and Applied Sciences**   _____

Prof. Dr. M. A. Sahir Arıkan
Head of the Department, **Mechanical Engineering**   _____

Prof. Dr. Süha Oral
Supervisor, **Mechanical Engineering Dept., METU**   _____

Examining Committee Members:

Assoc. Prof. Dr. Uğur Polat
Civil Engineering Dept., METU   _____

Prof. Dr. Süha Oral
Mechanical Engineering Dept., METU   _____

Prof. Dr. Can Çoğun
Mechatronics Engineering Dept., Çankaya University   _____

Prof. Dr. Müfit Gülgeç
Mechatronics Engineering Dept., Çankaya University   _____

Assoc. Prof. Dr. Hüsnü Dal
Mechanical Engineering Dept., METU   _____

Date: 21.02.2023

I hereby declare that all information in this document has been obtained and presented in accordance with academic rules and ethical conduct. I also declare that, as required by these rules and conduct, I have fully cited and referenced all material and results that are not original to this work.

Name, Last name: Suat ONTAÇ

Signature:

ABSTRACT

A PANEL FINITE ELEMENT WITH DISTORTIONAL MODES FOR THE ANALYSIS OF OPEN SECTION THIN WALLED BEAMS

Ontaç, Suat
Doctor of Philosophy, Mechanical Engineering
Supervisor: Prof. Dr. Süha Oral

February 2023, 64 pages

In this thesis, a panel finite element is developed for the analysis of the isotropic, open section, thin walled beams. In this study, the axial deformation, Euler-Bernoulli bending, Vlasov torsion and Kirchoff shell theories are combined to determine the displacements including in-plane and out-of-plane distortions in the cross sections of open section thin walled beams.

The open section thin walled beam element is obtained by the assembly of panel elements. This element has two nodes each having 15 degrees of freedom. A MATLAB computer code is developed for the panel finite element anaysis to calculate the displacements and stresses at any point in the beam. The results obtained are compared to the results taken from literature and ANSYS software.

Keywords: Open Section Thin Walled Beam, Panel Finite Element Method, Distortion

ÖZ

AÇIK KESİTLİ İNCE CİDARLI KİRİŞLERİN ANALİZİ İÇİN ÇARPILMA MODLARI İÇEREN BİR PANEL SONLU ELEMANI

Ontaç, Suat
Doktora, Makina Mühendisliği
Tez Yöneticisi: Prof. Dr. Süha Oral

Şubat 2023, 64 sayfa

Bu tezde, izotropik, açık kesitli, ince cidarlı kirişlerin analizi için bir panel sonlu elemanı geliştirilmiştir. Bu çalışmada, açık kesitli ince cidarlı kirişlerde, düzlem içi ve düzlem dışı çarpılmaları da içeren deplasmanları elde etmek için, eksenel deformasyon, Euler-Bernoulli eğilme, Vlasov burulma ve Kirchoff kabuk teorileri birleştirilmektedir.

Açık kesitli ince cidarlı çubuk elemanı panel elemanlarının birleştirilmesiyle elde edilmektedir. Bu eleman her biri 15 serbestlik derecesi bulunan iki düğüm noktasına sahiptir.

Bu çalışmada, kiriş üzerindeki herhangi bir noktada oluşan deplasman ve gerilim değerini hesaplayan bir MATLAB bilgisayar kodu geliştirilmiştir. Elde edilen sonuçlar literatürden ve ANSYS yazılımından alınan sonuçlarla karşılaştırılmıştır.

Anahtar Kelimeler: Açık Kesitli İnce Cidarlı Kiriş, Panel Sonlu Elemanlar Metodu, Çarpılma

To my mother and sister

ACKNOWLEDGMENTS

TABLE OF CONTENTS

LIST OF TABLES

TABLES

LIST OF FIGURES

FIGURES

LIST OF ABBREVIATIONS

ABBREVIATIONS

3D	:	3 Dimensional
DOF	:	Degree of Freedom
Eq.	:	Equation
FE	:	Finite Element
FEA	:	Finite Element Analysis
FEM	:	Finite Element Method
GBT	:	Generalized Beam Theory
NMM	:	Natural Modes Based Method
PFE	:	Panel Finite Element
SEM	:	Sonlu Eleman Metodu

LIST OF SYMBOLS

SYMBOLS

C	:	Centroid of a cross section
E	:	Modulus of elasticity
G	:	Shear modulus
I	:	Second moment of area
J	:	Polar moment of inertia
k	:	Panel stiffness matrix
k_σ	:	Panel stress stiffness matrix
O	:	Shear center
Q	:	First moment of area
γ	:	Shear strain
δ	:	Degrees of freedom vector
ε	:	Normal strain
π_p	:	Total potential energy of the panel
σ	:	Normal stress
τ	:	Shear stress
ω	:	Sectorial coordinate

CHAPTER 1

INTRODUCTION

1.1   Thesis Overview

A beam is called thin walled if its cross section consists of simply or multiply connected walls in which the wall thicknesses are very small compared to the dimensions of the cross section.

The thin walled beams are commonly used in engineering applications, such as aerospace structures, ship hulls, vehicle structures, bridges and various load carrying members due to their high stiffness-to-mass ratio and convenience to design and manufacture. Significant amount of material saving can be obtained if thin walled beams are used instead of solid or thick-walled beams.

The thin walled beam cross sections are represented by the centerlines of the walls which are called edges. The end points of an edge are called vertices. The section is called open section if the edges are simply connected, and closed section if the edges are multiply connected. In this thesis, only open section beams are studied.

The displacements of beams are the sum of rigid and elastic motions of the beam cross sections. In a solid section beam, the elastic motions are negligible and the displacements can accurately be defined in terms of the rigid motions. However, in a thin walled beam, the elastic motions cannot be neglected. Therefore, the kinematic behavior of solid and thin walled beams are considerably different and the conventional beam theories of Euler–Bernoulli and Timoshenko cannot be used to analyse thin walled structures accurately. In the Vlasov beam theory, the out-of-plane distortion in torsion is included but the in-plane distortions of the cross section are neglected.

1.2   Thesis Objective

The objective of this thesis is to develop a cost effective method for the analysis of open section thin walled beams by considering rigid, in-plane and out-of-plane elastic modes of deformation in the cross sections.

1.3   Thesis Scope

This thesis consists of five chapters. The starting chapter is Chapter 1 which introduce the study outline, thesis objective, and thesis scope. In Chapter 2, a literature survey which includes the previous studies is given. In Chapter 3, a panel finite element for open section thin walled beams is formulated. In Chapter 4, different test problems are solved and the results are compared with the shell solutions obtained from ANSYS commercial finite element analysis package. Chapter 5 is the conclusion for the present study and also contains recommendations for future work on this topic.

CHAPTER 2

LITERATURE REVIEW

The theory of thin walled beams have been subject to extensive research for years. Especially in the recent years, researches are focusing on the the cross section deformation including in-plane distortion. The other aim is minimizing the calculation time and effort for the analyses.

The first study for modelling the kinematics of thin walled beams was done by Vlasov [1]. He studied and developed the theory of sectorial area assuming the non-uniform torsion along the beam axis contributing to out-of-plane warping of the cross-section. In this theory, it is assumed that the cross-section is rigid in its own plane and there is no shear deformation along the profile mid-line.

The research community globally accepted Vlasov's analytical model and made some extention studies over the years in order to take into account for the other effects like geometric non-linearities in longitudinal deformations caused by large cross sectional rotation, shear deformations along the wall thickness, variable cross sections (stepped or tapered), curved axis beams or nonlinear warping effects.

Capurso [2] proposed a generalized description of warping and revised Vlasov theory so that shear deformation over the cross-section is included.

Schardt [3] proposed a generalized beam theory in which the in and out-of-plane distortions are considered. In this study, first-order analysis of prismatic members with thin walled simple open or cylindrical cross sections have been performed by superposing a number of cross-sectional natural modes whose magnitudes varies along the beam span. A second-order analysis for the generalized beam theory has also been presented by Schardt [4]. These studies have been translated into English in later years [5].

Andreassen [6] presented a novel mode-based method which considers the distortion of the cross section with a limited number of degrees of freedom by using a semi-discretized approach including the geometric stiffness terms.

Jönsson [7] made a study which generalizes the classical thin walled beam theory for open and closed cross sections to include one distortional deformation mode. For this purpose, distortional cross section parameters are defined and a normalization technique is introduced. Finally, the theoretical formulations for torsion and distortion are constructed and three different cross sections are illustrated in order to verify the method and show the effects of the theoretical parameters.

Hansen and Jönsson [8] introduced a novel one dimensional beam model in order to analyse deformable section thin walled beams. In this model, for the derivation of the three dimensional diplacement modes, the natural modes of the cross section are determined. This cross section determination process can be used to obtain both rigid body modes and distortions modes of the beam with exponential and polynomial variations along the beam span. All these displacement modes enable a formulation for an advanced thin walled beam element.

Zhang, Zhu, Ji and Peng [9] presented a simplified approach in order to identify the cross sectional deformation modes of prismatic thin walled structures. This provides the formation of a higher order beam model for the dynamic analyses. In this study, the displacement field is assumed as a linear superposition of basis functions whose amplitudes changes along the beam span. These basis functions are obtained from the nodal displacements of the beam cross section which is discretized on the midline, by using interpolating polynomials. In order to produce the primary deformation modes, the basis deformation modes are superposed. And then, the final set of the sectional deformation modes are assembled to the primary deformation modes which are used to update the basis functions in the higher order beam model.

Zhang, Ji and Zhu [10] presented an alternative approach to obtain the cross section deformation modes of a thin walled beam. In this study, the preliminary deformation

modes considering their participations in free vibration modes are assembled and integrated in the governing equations of higher order model.

Ghose [11] developed a three noded isoparametric beam finite element which is based on Benscoter theory. The autor states that the classical beam theories assume that the warping is proportional to the twist rate, while the Benscoter's theory assumes the warping is proportional to the warping function, which is an independent quantity. Also, the use of Benscoter's theory has an advantage since the effects of secondary shear strains are taken into consideration which are negligable in classsical beam theories.

Lin and Hsiao [12] develeoed an analytical formulation for torsional warping in order to analyse open-section thin walled beams. This analytical formulation is a combination of the Vlasov beam theory and Kirchhoff plate/shell theory. They emphasise that Vlasov and Timoshenko considered only primary warping, while, Goodier and Gjelsvik considered both primary and secondary warping. For this reason, they used Goodier's theory for the approximation of torsional warping of an open-section thin walled beam. The authors, then, constructed and presented a more general expression for the analysis of an open-section thin walled beam including the torsional warping.

Heo, Kim and Kim [13] showed that a distortional rigidity affects the cross section of a thin walled closed beam as well as torsional and bending rigidities. The autors states that there are many investigations in order to analyze distortional and warping deformations, but their article is perhaps the first study showing how the additional consideration of the distortional rigidity affects the design of the thin walled beam cross section shape.

Sapountzakis and Mokos [14] presented the dynamic analysis of 3-dimensional beam elements which are fixed at their edges and under distributed dynamic twisting, bending, transverse and longitudinal loading. For this purpose, a boundary element method is developed for the beam element stiffness matrix, which is a 14x14 matrix and is taking the warping and shear deformation effects into consideration. Free and

forced transverse vibrations and longitudinal or torsional vibrations are considered, taking the transverse, longitudinal, rotatory, torsional and warping inertia and damping resistance into account. Also, especially, the influence of the warping effect is examined in open form cross sections.

Murin and Kutis [15] developed a finite element with constant stiffness for the analysis of open and closed section thin walled beams including torsion with warping. In this study, the local element stiffness matrix is derived by using the torsion with warping and the second order beam theory including the deformations due to shear. The warping part of the first derivative of the twist angle are added to the degree of freedom vector in each node of the beam finite element.

Li and Luo [16] derived a stiffness matrix of a thin walled beam element considering the distortion effects by using generalized coordinate method and stationary principle potential energy. The autors developed a finite element program for computing the thin walled box steel beams by using the derived stiffness matrix. This program takes the section distortion and warping effects into consideration and analyses the influences and the distributions of the stresses occured.

Ferradi, Cespedes and Arquier [17] presented a new beam finite element including an accurate representation of normal stresses caused by shear lag or restrained torsion. Warping modes are superposed in order to represent cross-section warping and are defined as warping functions for the kinematics of the beam. The exact solution of the equilibrium equations is presented for a predetermined number of warping modes while the elastic deformations are mesh-independent totally.

Genoese, Genoese, Bilotta and Garcea [18] presented a linear model for thin walled beams with heterogeneous anisotropic materials. The autor uses Ritz-Galerkin approximation using independent description of displacement and stress fields. These fields are obtained from a preliminary semi-analytical solution based on a finite element formulation of the beam cross section. The displacement and stress definition includes both the generalized Saint Venant solution and additional effects due to out-of-plane warping and cross section distortions.

Vieira, Virtuoso and Pereira [19] presented a higher order model for the prismatic thin walled structures considering the cross section warping together with the cross section in-plane flexural deformation. In this model, the displacement field on the beam cross section is considered as a set of linear independent basis functions. The beam governing equations are derived considering the displacement field assumption and causing a set of 4th order differential system of equations.

Gao [20] developed a 3-dimensional beam finite element with deformable cross section adding the strain components neglected in the beam theories so that the 3-dimensional stress/strain constitutive relations are to be applicable.

Garcea, Gonçalves, Bilotta, Manta, Bebiano, Leonetti, Magisano and Camotim [21] compared two approaches, which are the method of generalized eigenvectors and the generalized beam theory in order to obtain the cross section deformation modes of deformable section thin walled beams. In this comparison, the autors reviewed both approaches, underlying their similarities and differences.

Latalski and Zulli [22] studied curvilinear cross section thin walled beams by defining the kinematic properties of the walls and made an assumption that the displacement of a point on the wall is a linear combination of unknown amplitudes and preformed trial in-plane and out-of-plane warping functions. Then, they derived the governing equations by using Hamilton's method and compared the analytical results to the results of finite element analysis.

Kim, Choi, Kim and Jang [23] are presented a new systematic approach in order to obtain the deformation modes of an arbitrary thin walled beam cross section in the frame of the higher order beam theory. Warping and distortion modes are derived from the lowest mode set as a new higher order mode set. Warping modes are derived from the shear stress of in-plane modes, distortion modes are derived from out-of-plane modes by using the Poisson's effect. The autors built the higher order modes as a combination of the integrated functions of lower order modes.

CHAPTER 3

PANEL FINITE ELEMENT

3.1   Introduction

Consider an open section thin walled beam along the beam axis x. The cross sectional coordinate system are shown in Fig-3.1 where the dashed line represents the wall centerline of an edge. (y, z) are the Cartesian coordinates. The centroid and shear center of the cross section are $C(0,0)$ and $O(y_o, z_o)$, respectively. (s, n) are the edge coordinates, and ω is the sectorial coordinate of a point b with respect to point a on the wall centerline. xyz, xsn are right handed coordinate systems.
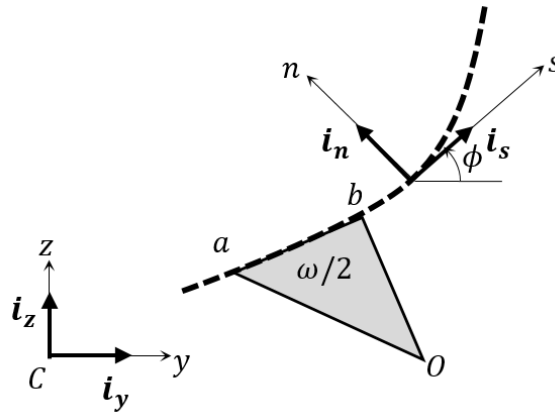
Figure 3.1. Coordinate systems of a thin walled beam

The transformation between yz and sn is

$$\begin{bmatrix} y \\ z \end{bmatrix} = \begin{bmatrix} y_i \\ z_i \end{bmatrix} + \begin{bmatrix} cos\phi & -sin\phi \\ sin\phi & cos\phi \end{bmatrix} \begin{bmatrix} s \\ n \end{bmatrix} \tag{3.1}$$

The beam displacements at a point (x, y, z) are $U_x(x, y, z)$, $U_y(x, y, z)$ and $U_z(x, y, z)$. U_x, U_y, U_z can be expressed as a combination of the rigid

and elastic deformation modes of the cross section. The displacements on the beam axis are $u_x(x) = U_x(x, 0,0), u_y(x) = U_y(x, 0,0), u_z(x) = U_z(x, 0,0)$. The rotations of a cross section at x are $\theta_x(x), \theta_y(x) = -u_z{}'(x), \theta_z(x) = u_y{}'(x)$ about x, y, z axes.

3.1.1   Euler-Bernoulli Theory

In the Euler-Bernoulli theory, the displacements are assumed as

$$U_x(x, y, z) = u_x(x) - yu_y'(x) - zu_z{}'(x)$$

$$U_y(x, y, z) = u_y(x) - (z - z_o)\theta_x(x) \tag{3.2}$$

$$U_z(x, y, z) = u_z(x) + (y - y_o)\theta_x(x)$$

where u_x, u_y, u_z are due to rigid translations of the cross section in x, y, z directions, $-yu_y', -zu_z'$ are due to rigid rotations of the cross section about z, y axes, $-(z - z_o)\theta_x, (y - y_o)\theta_x$ are due to rigid rotation of the cross section about x axis. It is seen that the displacement field of the Euler-Bernoulli theory is based on rigid modes only.

3.1.2   Axial Deformation and Bending

The governing equation of axial deformation is

$$EAu_x'' + f_x = 0 \tag{3.3}$$

The governing equations of bending in the Euler-Bernoulli beam theory are

$$E(I_yI_z - I_{yz}{}^2)u_y{}^{iv} = I_yf_y + I_{yz}f_z$$

$$E(I_yI_z - I_{yz}{}^2)u_z{}^{iv} = I_zf_z + I_{yz}f_y \tag{3.4}$$

where f_x, f_y, f_z are the intensities of distributed loads in x, y, z directions.

The normal stress in axial loading is

$$\sigma_x = \frac{N}{A} \tag{3.5}$$

where

$$A = \int_c t\,ds \quad N = EAu'_x \tag{3.6}$$

The normal stress in bending is

$$\sigma_x = \frac{1}{I_y I_z - I_{yz}{}^2}\left[\left(I_{yz}M_y - I_y M_z\right)y + \left(I_z M_y - I_{yz}M_z\right)z\right] \tag{3.7}$$

where

$$I_y = \int_c z^2 t\,ds$$

$$I_z = \int_c y^2 t\,ds \tag{3.8}$$

$$I_{yz} = -\int_c yzt\,ds$$

$$M_y = E\left(I_{yz}u_y'' - I_y u_z''\right)$$

$$\tag{3.9}$$

$$M_z = E\left(I_z u_y'' - I_{yz}u_z''\right)$$

The shear stress in bending is

$$\tau_{xs} = -\frac{1}{t\left(I_y I_z - I_{yz}{}^2\right)}\left[\left(I_z S_z + I_{yz}S_y\right)Q_y + \left(I_y S_y + I_{yz}S_z\right)Q_z\right] \tag{3.10}$$

where

10

$$S_y = -M_z'$$

$$(3.11)$$

$$S_z = M_y'$$

$$Q_y = \int ztds$$

$$(3.12)$$

$$Q_z = \int ytds$$

3.1.3 Vlasov Theory

The above treatment are valid in the Vlasov beam theory. However, the torsional deformation is formulated by including the effect of warping which is the out-of-plane distortion of the cross section under torsional loads and this effect is much more pronounced in thin walled sections compared to that in solid sections.

In this case, the displacements along an edge are assumed as

$$U_x(x,s) = u_x(x) - y(s)u_y'(x) - z(s)u_z{}'(x) + \omega(s)\theta_x{}'(x)$$

$$U_y(x,s) = u_y(x) - (z(s) - z_o)\theta_x(x) \qquad (3.13)$$

$$U_z(x,s) = u_z(x) + (y(s) - y_o)\theta_x(x)$$

where ω is the warping function and $\omega\theta_x{}'$ is the warping displacement in torsion. In this case, the cross section does not remain plane but distorts in x-direction. Therefore, this is an elastic mode.

3.1.4   Torsion

Under torsional loads, a section at x twists about the shear center $O(y_o, z_o)$ by a twist angle $\theta_x(x)$ and undergoes warping $U_x(x, y, z)$.
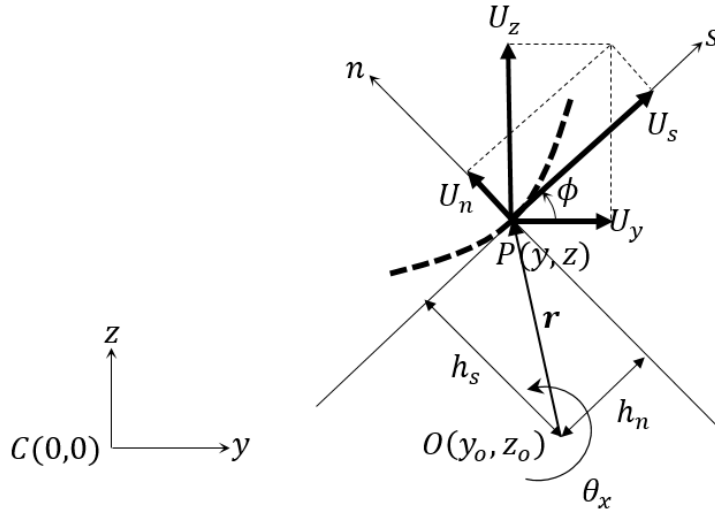
Figure 3.2. Out-of-plane distortion in torsion

The transverse displacement during twisting is

$$\boldsymbol{\delta_P} = \theta_x \boldsymbol{i_x} \times \boldsymbol{r} = U_y \boldsymbol{i_y} + U_z \boldsymbol{i_z} \tag{3.14}$$

where

$$\boldsymbol{r} = (y - y_o)\boldsymbol{i_y} + (z - z_o)\boldsymbol{i_z} \tag{3.15}$$

$$U_y = -(z - z_o)\theta_x$$

$$\tag{3.16}$$

$$U_z = (y - y_o)\theta_x$$

The displacements in sn are

$$\begin{bmatrix} U_s \\ U_n \end{bmatrix} = \begin{bmatrix} cos\phi & sin\phi \\ -sin\phi & cos\phi \end{bmatrix} \begin{bmatrix} U_y \\ U_z \end{bmatrix} \tag{3.17}$$

Define

$$h_s = \boldsymbol{r} \cdot \boldsymbol{i}_n \tag{3.18}$$

Then

$$U_s = -h_s \theta_x \tag{3.19}$$

The shear strain is

$$\gamma_{xs} = \frac{\partial U_x}{\partial s} + \frac{\partial U_s}{\partial x} = \frac{\partial U_x}{\partial s} - h_s \theta_x' \tag{3.20}$$

Then

$$\frac{\partial U_x}{\partial s} = \gamma_{xs} - \frac{\partial U_s}{\partial x} = \frac{\tau_{xs}}{G} + h_s \theta_x' \ \rightarrow U_x = \theta_x' \int h_s ds \tag{3.21}$$

since $\int \tau_{xs} ds = 0$ in open sections where τ_{xs} varies linearly along n-axis and is zero along the wall centerline. U_x can be written as

$$U_x = \omega \theta_x' \tag{3.22}$$

Where

$$\omega(s) = \int h_s ds \tag{3.23}$$

is the warping function.

The governing equation of torsion is

$$EI_w \theta_x{}^{iv} - GJ\theta_x'' = m_x \tag{3.24}$$

where m_x is the intensity of distributed torque.

The resultant of the shear stresses in twisting is the St.Venant torque T_s. Normal and additional shear stresses are caused by warping if $\theta_x' \neq 0$. Resultant of normal and shear stresses in warping are the warping moment M_w and the warping torque T_w.

The shear stress in warping is

$$\tau_{xs} = -\frac{2T_s}{J}n \tag{3.25}$$

where

$$J = \frac{1}{3}\sum_{n=1}^{N} L_n t_n^3 \tag{3.26}$$

$$T_s = GJ\theta_x' \tag{3.27}$$

The normal stress in warping is

$$\sigma_x = \frac{M_w}{I_w}\omega \tag{3.28}$$

where

$$I_w = \int_A \omega^2 t \, ds \tag{3.29}$$

$$M_w = EI_w\theta_x'' \tag{3.30}$$

The shear stress in warping is

$$\tau_{xs} = \frac{T_w}{I_w t}Q_\omega \tag{3.31}$$

where

$$Q_\omega = \int \omega t \, ds \tag{3.32}$$

$$T_w = -EI_w\theta''' \tag{3.33}$$

3.2   Panel Finite Element Formulation

The thin walled beams are shell structures and the most accurate results are obtained by the shell finite element models. However, the shell analysis is prohibitively costly and a special thin walled beam element is a necessity. The Vlasov beam element is a good approximation. However, it neglects the elastic modes other than torsional warping. Its accuracy can be improved by considering the elastic modes under other loading conditions. This is accomplished by studying shell deformations under axial and flexural loadings and additional elastic modes are added to the beam displacement field.

3.2.1.1   Axial Loading
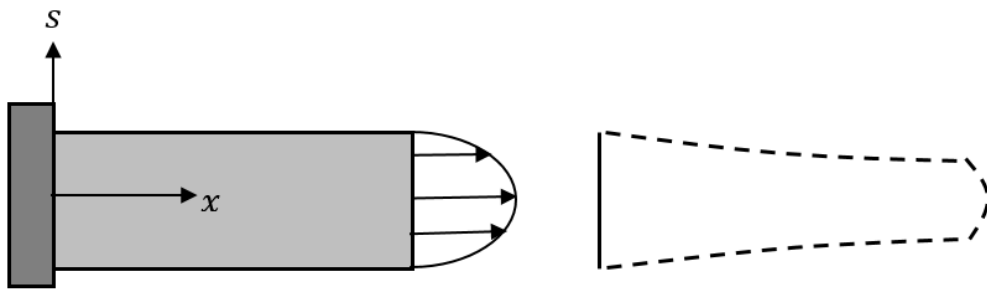
Figure 3.3. Axial loading elastic modes

The necessary elastic modes are

$$s^2 U_x^{ss} \rightarrow y^2 u_x^{yy} + z^2 u_x^{zz}$$

$$s U_s^s \rightarrow y u_y^y, z u_z^z$$

(3.34)

for U_x and U_s, respectively.

15

3.2.1.2   In-plane Bending
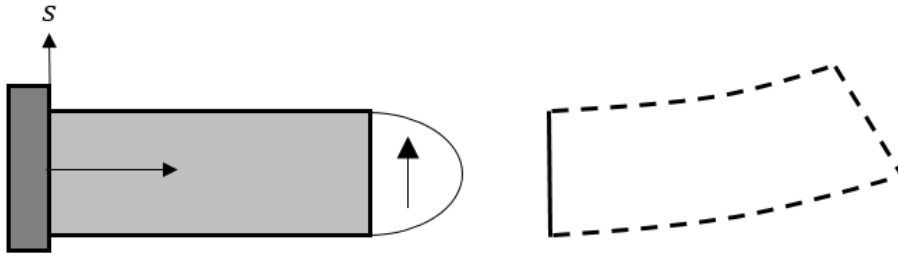
Figure 3.4. In-plane transverse loading elastic modes

In this case, rigid modes give sufficiently accurate results and elastic modes are not necessary.

3.2.1.3   Out-of-plane Bending
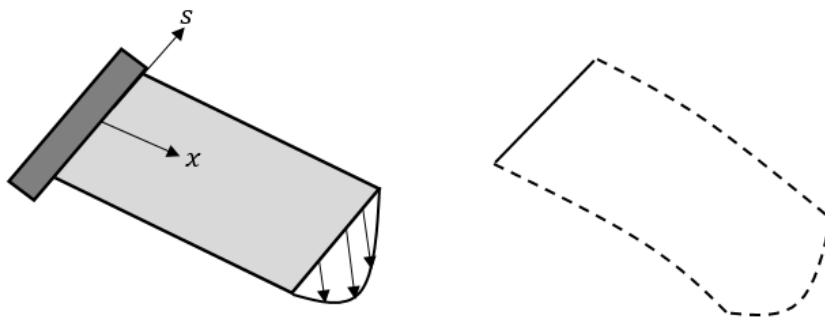
Figure 3.5. Out-of-plane transverse loading elastic modes

An elastic mode

$$s^2 U_n^{ss} \rightarrow y^2 u_y^{yy} + z^2 u_y^{zz}, y^2 u_z^{yy} + z^2 u_z^{zz} \tag{3.35}$$

is necessary for U_n.

Then, the Vlasov displacements can be modified as

$$U_x(x,s) = u_x(x) - y(s)u_y'(x) - z(s)u_z'(x) + \omega(s)\theta_x'(x)$$
$$+ y^2(s)u_x^{yy}(x) + z^2(s)u_x^{zz}(x)$$

(3.36)

$$U_y(x,s) = u_y(x) - [z(s) - z_o]\theta_x(x) + y(s)u_y^y(x) + y^2(s)u_y^{yy}(x)$$
$$+ z^2(s)u_y^{zz}(x)$$

(3.37)

$$U_z(x,s) = u_z(x) + [y(s) - y_o]\theta_x(x) + z(s)u_z^z(x) + y^2(s)u_z^{yy}(x)$$
$$+ z^2(s)u_z^{zz}(x)$$

(3.38)

In this study, a thin walled beam is divided into beam finite elements along the beam axis and each beam element is divided into panel finite elements along the contour of the cross section. The number of element degrees of freedom is independent of the number of panels. Consider a rectangular panel of a thin walled beam. $C(0,0)$ is the centroid and $O(y_o, z_o)$ is the shear center of the beam cross section.
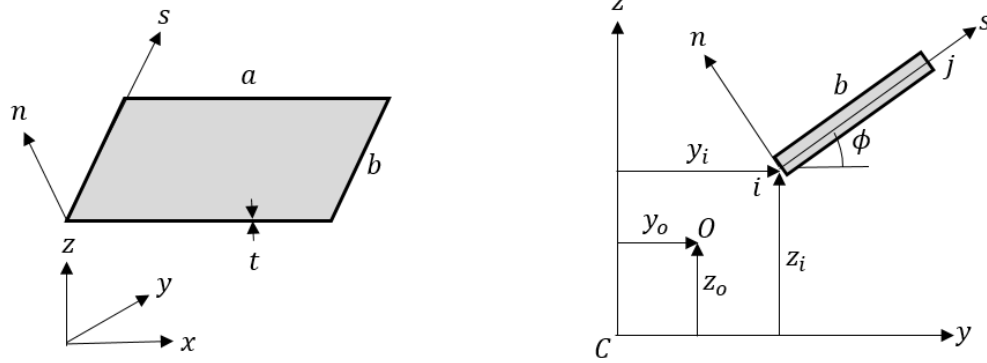
Figure 3.6. A panel element ij of beam element and its coordinates

Define

$$p = cos\phi = \frac{y_j - y_i}{b}$$

(3.39)

$$q = sin\phi = \frac{z_j - z_i}{b}$$

(3.40)

$$r = \frac{\omega_j - \omega_i}{b}$$

(3.41)

Then

$$\begin{bmatrix} y \\ z \end{bmatrix} = \begin{bmatrix} y_i \\ z_i \end{bmatrix} + \begin{bmatrix} p & -q \\ q & p \end{bmatrix} \begin{bmatrix} s \\ n \end{bmatrix}$$

(3.42)

$$\begin{bmatrix} s \\ n \end{bmatrix} = \begin{bmatrix} p & q \\ -q & p \end{bmatrix} \begin{bmatrix} y - y_i \\ z - z_i \end{bmatrix}$$

At the wall centerline:

$$y = y_i + ps$$

$$z = z_i + qs$$

(3.43)

$$\omega = \omega_i + rs$$

Assume the displacements as

$$u_x = \boldsymbol{\phi} \boldsymbol{d}_{u_x} \quad u_y = \boldsymbol{\varphi} \boldsymbol{d}_{u_y} \quad u_z = \boldsymbol{\varphi} \boldsymbol{d}_{u_z} \quad \theta_x = \boldsymbol{\varphi} \boldsymbol{d}_{\theta_x}$$

$$u_x^{yy} = \boldsymbol{\phi} \boldsymbol{d}_{u_x^{yy}} \quad u_x^{zz} = \boldsymbol{\phi} \boldsymbol{d}_{u_x^{zz}}$$

(3.44)

$$u_y^y = \boldsymbol{\phi} \boldsymbol{d}_{u_y^y} \quad u_y^{yy} = \boldsymbol{\phi} \boldsymbol{d}_{u_y^{yy}} \quad u_y^{zz} = \boldsymbol{\phi} \boldsymbol{d}_{u_y^{zz}}$$

$$u_z^z = \boldsymbol{\phi} \boldsymbol{d}_{u_z^z} \quad u_z^{yy} = \boldsymbol{\phi} \boldsymbol{d}_{u_z^{yy}} \quad u_z^{zz} = \boldsymbol{\phi} \boldsymbol{d}_{u_z^{zz}}$$

where

$$\boldsymbol{\phi} = \frac{1}{a} [(a - x) \quad x]$$

(3.45)

$$\boldsymbol{\varphi} = \frac{1}{a^3} [(a + 2x)(a - x)^2 \quad ax(a - x)^2 \quad x^2(3a - 2x) \quad ax^2(x - a)]$$ (3.46)

and

18

$$d_{u_x} = \begin{bmatrix} u_{x1} \\ u_{x2} \end{bmatrix} \qquad d_{u_y} = \begin{bmatrix} u_{y1} \\ u_{y1}' \\ u_{y2} \\ u_{y2}' \end{bmatrix} \qquad d_{u_z} = \begin{bmatrix} u_{z1} \\ u_{z1}' \\ u_{z2} \\ u_{z2}' \end{bmatrix} \qquad d_{\theta_x} = \begin{bmatrix} \theta_{x1} \\ \theta_{x1}' \\ \theta_{x2} \\ \theta_{x2}' \end{bmatrix}$$

$$d_{u_x^{yy}} = \begin{bmatrix} u_{x1}^{yy} \\ u_{x2}^{yy} \end{bmatrix} \qquad d_{u_x^{zz}} = \begin{bmatrix} u_{x1}^{zz} \\ u_{x2}^{zz} \end{bmatrix}$$

$$d_{u_y^y} = \begin{bmatrix} u_{y1}^y \\ u_{y2}^y \end{bmatrix} \qquad d_{u_y^{yy}} = \begin{bmatrix} u_{y1}^{yy} \\ u_{y2}^{yy} \end{bmatrix} \qquad d_{u_y^{zz}} = \begin{bmatrix} u_{y1}^{zz} \\ u_{y2}^{zz} \end{bmatrix}$$

$$d_{u_z^z} = \begin{bmatrix} u_{z1}^z \\ u_{z2}^z \end{bmatrix} \qquad d_{u_z^{yy}} = \begin{bmatrix} u_{z1}^{yy} \\ u_{z2}^{yy} \end{bmatrix} \qquad d_{u_z^{zz}} = \begin{bmatrix} u_{z1}^{zz} \\ u_{z2}^{zz} \end{bmatrix}$$

(3.47)

Define

$$\begin{aligned} d = [& u_{x1} \quad u_{y1} \quad u_{z1} \quad \theta_{x1} \quad \theta_{y1} \quad \theta_{z1} \quad \theta_{x1}' \quad \dots \\ & u_{x1}^{yy} \quad u_{x1}^{zz} \quad u_{y1}^y \quad u_{y1}^{yy} \quad u_{y1}^{zz} \quad u_{z1}^z \quad u_{z1}^{yy} \quad u_{z1}^{zz} \quad \dots \\ & u_{x2} \quad u_{y2} \quad u_{z2} \quad \theta_{x2} \quad \theta_{y2} \quad \theta_{z2} \quad \theta_{x2}' \quad \dots \\ & u_{x2}^{yy} \quad u_{x2}^{zz} \quad u_{y2}^y \quad u_{y2}^{yy} \quad u_{y2}^{zz} \quad u_{z2}^z \quad u_{z2}^{yy} \quad u_{z2}^{zz}] \end{aligned}$$

(3.48)

Then

$$\begin{bmatrix} U_x \\ U_y \\ U_z \end{bmatrix} = \begin{bmatrix} \boldsymbol{\Omega}_x \\ \boldsymbol{\Omega}_y \\ \boldsymbol{\Omega}_z \end{bmatrix} d$$

(3.49)

The displacements in xsn are

$$\begin{bmatrix} U_x \\ U_s \\ U_n \end{bmatrix} = \begin{bmatrix} 1 & 0 & 0 \\ 0 & p & q \\ 0 & -q & p \end{bmatrix} \begin{bmatrix} U_x \\ U_y \\ U_z \end{bmatrix} = \begin{bmatrix} 1 & 0 & 0 \\ 0 & p & q \\ 0 & -q & p \end{bmatrix} \begin{bmatrix} \boldsymbol{\Omega}_x \\ \boldsymbol{\Omega}_y \\ \boldsymbol{\Omega}_z \end{bmatrix} d = \begin{bmatrix} \boldsymbol{\Omega}_x \\ \boldsymbol{\Omega}_s \\ \boldsymbol{\Omega}_n \end{bmatrix} d = \boldsymbol{\Omega} d$$

(3.50)

In the panel finite element, shell strain definitions are used:

$$\varepsilon_x = \frac{\partial U_x}{\partial x} - n\frac{\partial^2 U_n}{\partial x^2}$$

$$\varepsilon_s = \frac{\partial U_s}{\partial s} - n\frac{\partial^2 U_n}{\partial s^2} \qquad (3.51)$$

$$\gamma_{xs} = \frac{\partial U_x}{\partial s} + \frac{\partial U_s}{\partial x} - 2n\frac{\partial^2 U_n}{\partial x\partial s}$$

Then

$$\boldsymbol{\varepsilon} = \begin{bmatrix} \varepsilon_x \\ \varepsilon_s \\ \gamma_{xs} \end{bmatrix} = \begin{bmatrix} \dfrac{\partial}{\partial x} & 0 & -n\dfrac{\partial^2}{\partial x^2} \\[2mm] 0 & \dfrac{\partial}{\partial s} & -n\dfrac{\partial^2}{\partial s^2} \\[2mm] \dfrac{\partial}{\partial s} & \dfrac{\partial}{\partial x} & -2n\dfrac{\partial^2}{\partial x\partial s} \end{bmatrix}\boldsymbol{\Omega d} = \boldsymbol{Bd} \qquad (3.52)$$

The total potential energy of the panel is

$$\pi_p = \frac{1}{2}\int_V \boldsymbol{\varepsilon}^T\boldsymbol{C}\boldsymbol{\varepsilon}\,dV - \int_o^a \boldsymbol{u}^T\boldsymbol{p}\,dx = \frac{1}{2}\int_V \boldsymbol{d}^T\boldsymbol{B}^T\boldsymbol{C}\boldsymbol{B}\boldsymbol{d}\,dV - \int_0^a \boldsymbol{d}^T\boldsymbol{\Omega}^T\boldsymbol{p}\,dx \qquad (3.53)$$

where $\boldsymbol{p}$ is the intensity of distributed loading and

$$\boldsymbol{C} = \frac{E}{1-v^2}\begin{bmatrix} 1 & v & 0 \\ v & 1 & 0 \\ 0 & 0 & \dfrac{1-v}{2} \end{bmatrix} \qquad (3.54)$$

is the material matrix. Define

$$\boldsymbol{k}_p = \int_V \boldsymbol{B}^T\boldsymbol{C}\boldsymbol{B}\,dV = \int_0^a\int_0^b\int_{-t/2}^{t/2} \boldsymbol{B}^T\boldsymbol{C}\boldsymbol{B}\,dn\,ds\,dx \qquad (3.55)$$

$$\boldsymbol{f}_p = \int_{A_f} \boldsymbol{\Omega}^T\boldsymbol{p}\,dx \qquad (3.56)$$

20

where $\boldsymbol{k}_p$ is the stiffness matrix, and $\boldsymbol{f}_p$ is the force vector of the panel. Then

$$\pi_p = \frac{1}{2}\boldsymbol{d}^T \boldsymbol{k}_p \boldsymbol{d} - \boldsymbol{d}^T \boldsymbol{f}_p \qquad (3.57)$$

Consider a case in which a beam is initially stressed by an axial force and is subjected to flexural and/or torsional loads. Let the initial stresses be σ_{x0}, σ_{s0} and τ_{xs0}. A stress stiffness matrix is necessary to determine the effect of the axial force in flexural and/or torsional response. It is obtained by evaluating the work done by the membrane forces during transverse displacements. In the present case, the transverse displacement is U_n and the associated membrane strains are the quadratic Green strains which are:

$$\varepsilon_x = \frac{1}{2}\left(\frac{\partial U_n}{\partial x}\right)^2$$

$$\varepsilon_s = \frac{1}{2}\left(\frac{\partial U_n}{\partial s}\right)^2 \qquad (3.58)$$

$$\gamma_{xs} = \frac{\partial U_n}{\partial x}\frac{\partial U_n}{\partial s}$$

Then, the work done by the initial stresses is

$$\pi_{p0} = \int_V (\varepsilon_x \sigma_{x0} + \varepsilon_s \sigma_{s0} + \gamma_{xs}\tau_{xs0})dV$$

$$= \frac{1}{2}\int_V \begin{bmatrix} \partial U_n/\partial x \\ \partial U_n/\partial s \end{bmatrix}^T \begin{bmatrix} \sigma_{x0} & \tau_{xs0} \\ \tau_{xs0} & \sigma_{s0} \end{bmatrix} \begin{bmatrix} \partial U_n/\partial x \\ \partial U_n/\partial s \end{bmatrix} dV = \frac{1}{2}\int_V \boldsymbol{g}^T \boldsymbol{\lambda} \boldsymbol{g} dV \qquad (3.59)$$

$\boldsymbol{g}$ can be expressed as $\boldsymbol{g} = \boldsymbol{G}\boldsymbol{d}$.

Then

$$\pi_{p0} = \frac{1}{2} \int_V d^T G^T \lambda G d \, dV = \frac{1}{2} d^T k_\sigma d \tag{3.60}$$

where

$$k_{\sigma p} = \int_V G^T \lambda G \, dV = \int_0^a \int_0^b \int_{-t/2}^{t/2} G^T \lambda G \, dn \, ds \, dx \tag{3.61}$$

is the stress stiffness matrix of the panel and

$$\pi_{p0} = \frac{1}{2} d^T k_{\sigma p} d \tag{3.62}$$

The stiffness matrix and force vector of a beam element consisting of M_p panels are obtained by assembling the panel stiffness matrices and force vectors as

$$k = \sum_{i=1}^{M_p} k_{p_i} \qquad k_\sigma = \sum_{i=1}^{M_p} k_{\sigma p_i} \qquad f = f_{PF} + \sum_{i=1}^{M_p} f_{p_i} \tag{3.63}$$

where f_{PF} is the force vector due to point forces $F_x, F_y, F_z, T, M_y, M_z$ as

$$f_{PF} = F_x \Omega_x^T + F_y \Omega_y^T + F_z \Omega_z^T + T \Omega_{\theta_x}^T - M_y \Omega_z'^T + M_z \Omega_y'^T \tag{3.64}$$

and Ω_{θ_x} is δ_{θ_x} expanded to (1×15) size.

Then, the matrices and vectors of a beam having M_e elements and N nodes are assembled as

$$K = \sum_{i=1}^{M_e} k_i \qquad K_\sigma = \sum_{i=1}^{M_e} k_{\sigma i} \qquad F = \sum_{i=1}^{N} f_i \qquad D = \sum_{i=1}^{N} d_i \tag{3.65}$$

Note that the total potential energy of the beam is

22

$$\Pi = \sum_{j=1}^{M_e} \sum_{i=1}^{M_p} \left(\pi_{p_i} + \pi_{p0_i}\right)_j = \frac{1}{2} \boldsymbol{D}^T (\boldsymbol{K} + \boldsymbol{K}_\sigma) \boldsymbol{D} - \boldsymbol{D}^T \boldsymbol{F} \tag{3.66}$$

Setting the first variation $\delta\Pi = (\partial\Pi/\partial\boldsymbol{D})\delta\boldsymbol{D} = 0$, the panel equilibrium equations are obtained as

$$(\boldsymbol{K} + \boldsymbol{K}_\sigma)\boldsymbol{D} = \boldsymbol{F} \tag{3.67}$$

3.2.1.4   Stress   Calculation

The normal stresses and the shear stress due to St.Venant torque and the elastic modes can be calculated as

$$\begin{bmatrix} \sigma_x \\ \sigma_s \\ \tau_{xs} \end{bmatrix} = \boldsymbol{CBd} \tag{3.68}$$

The expressions for shear stresses due to transverse shear forces and the warping torque contain the third derivatives $u_y''', u_z''', \theta'''$ which do not appear in the formulation. Therefore, they must be calculated separately for each panel as follows:

3.2.1.4.1 τ_{xs} due to transverse shear forces

$$
\begin{aligned}
(\tau_{xs})_S &= \frac{E}{t}\left(Q_z u_y''' + Q_y u_z'''\right) \\[2mm]
&= \frac{EQ_z}{a^3 t}\begin{bmatrix} 12 & 6a & -12 & 6a \end{bmatrix}\begin{bmatrix} u_{y1} \\ \theta_{z1} \\ u_{y2} \\ \theta_{z2} \end{bmatrix} \\[2mm]
&+ \frac{EQ_y}{a^3 t}\begin{bmatrix} 12 & -6a & -12 & -6a \end{bmatrix}\begin{bmatrix} u_{z1} \\ \theta_{y1} \\ u_{z2} \\ \theta_{y2} \end{bmatrix}
\end{aligned}
\tag{3.69}
$$

3.2.1.4.2 τ_{xs} due to warping torque

$$(\tau_{xs})_{T_w} = -\frac{E}{t}Q_\omega\theta''' = -\frac{EQ_\omega}{a^3 t}[12 \quad 6a \quad -12 \quad 6a]\begin{bmatrix}\theta_{x1}\\\theta_{x1}'\\\theta_{x2}\\\theta_{x2}'\end{bmatrix} \tag{3.70}$$

where

$$Q_y = \int_0^s (z_i + qs)t\,ds$$

$$Q_z = \int_0^s (y_i + ps)t\,ds \tag{3.71}$$

$$Q_\omega = \int_0^s (\omega_i + rs)t\,ds$$

24

CHAPTER 4

NUMERICAL EXAMPLES

In this section, numerical test problems are given in order to compare the results of the panel finite element (PFE) method with those of ANSYS shell models and the beam theories. The panel finite element is implemented as a MATLAB code.

In the first five examples, PFE is tested against analytical beam results and a single ANSYS shell element solution to validate the shell-like behavior of the present element. The remaining four examples are thin walled beams with different sections under different loading conditions. The results obtained by PFE are compared with ANSYS shell models with fine mesh.

In the given examples, the dimensions are in millimeters (mm), the forces are in Newton (N) and the stresses are in Megapascal (MPa) unless otherwise specified.

4.1 Example-1

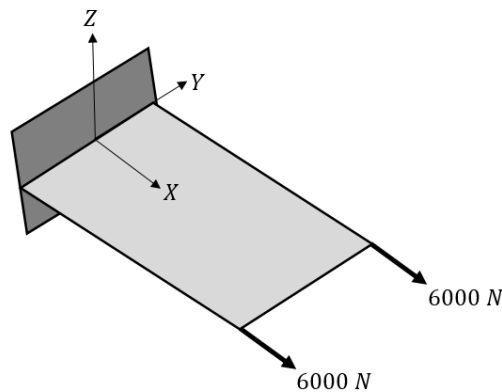$300\ mm \times 100\ mm \times 2\ mm\ plate, E = 200000\ N/mm^2, v = 0.3$

Figure 4.1. Example-1 Graphical Representation

This is an axial deformation problem. In the following, the results obtained by a single PFE are compared with the beam solution and a single ANSYS shell finite element. The beam solution gives U_x and σ_x only. ANSYS and PFE give $U_x, U_y, \sigma_x, \sigma_y, \tau_{xy}$.

Table 4.1. Displacements at $X = 300\ mm\ and\ Y = -50\ mm$ for Example-1

	U_x	U_y
Beam Theory	0.090000	0.0
ANSYS Shell Element	0.095863	0.005285
Panel Finite Element	0.095338	0.007168

Table 4.2. Displacements at $X = 300\ mm\ and\ Y = 0\ mm$ for Example-1

	U_x	U_y
Beam Theory	0.090000	0.0
ANSYS Shell Element	0.085794	0.0
Panel Finite Element	0.084858	0.0

Table 4.3. Displacements at $X = 300\ mm\ and\ Y = 50\ mm$ for Example-1

	U_x	U_y
Beam Theory	0.090000	0.0
ANSYS Shell Element	0.095863	-0.005285
Panel Finite Element	0.095338	-0.007168

Table 4.4. Stresses at $X = 0\ mm, Y = -50\ mm\ and\ Z = 0\ mm$ for Example-1

	σ_x	σ_s	τ_{xs}
Beam Theory	60.00	0.0	0.0
ANSYS Shell Element	60.01	12.53	3.46
Panel Finite Element	69.84	20.95	1.84

Table 4.5. Stresses at $X = 0\ mm, Y = 0\ mm\ and\ Z = 0\ mm$ for Example-1

	σ_x	σ_s	τ_{xs}
Beam Theory	60.00	0.0	0.0
ANSYS Shell Element	60.01	12.53	0.0
Panel Finite Element	62.17	18.65	0.0

Table 4.6. Stresses at $X = 0\ mm, Y = 50\ mm\ and\ Z = 0\ mm$ for Example-1

	σ_x	σ_s	τ_{xs}
Beam Theory	60.00	0.0	0.0
ANSYS Shell Element	60.01	12.53	-3.46
Panel Finite Element	69.84	20.95	-1.84

Table 4.7. Stresses at $X = 150\ mm, Y = -50\ mm\ and\ Z = 0\ mm$ for Example-1

	σ_x	σ_s	τ_{xs}
Beam Theory	60.00	0.0	0.0
ANSYS Shell Element	60.01	1.95	-14.13
Panel Finite Element	65.12	5.20	-14.29

Table 4.8. Stresses at $X = 150\ mm, Y = 0\ mm\ and\ Z = 0\ mm$ for Example-1

	σ_x	σ_s	τ_{xs}
Beam Theory	60.00	0.0	0.0
ANSYS Shell Element	60.01	1.95	0.0
Panel Finite Element	57.44	2.90	0.0

Table 4.9. Stresses at $X = 150\ mm, Y = 50\ mm\ and\ Z = 0\ mm$ for Example-1

	σ_x	σ_s	τ_{xs}
Beam Theory	60.00	0.0	0.0
ANSYS Shell Element	60.01	1.95	14.13
Panel Finite Element	65.12	5.20	14.29

4.2 Example-2

$300 \times 100 \times 2\ mm\ plate, E = 200000\ N/mm^2, v = 0.3$
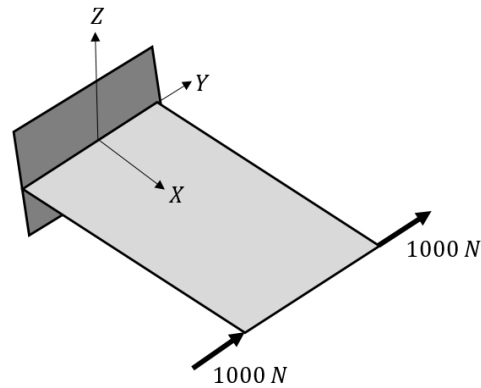

Figure 4.2. Example-2 Graphical Representation

This is an in-plane bending problem. In the following, the results obtained by a single PFE are compared with the beam solution and a single ANSYS shell finite element. The beam solution gives U_x, U_y and σ_x, τ_{xy}. ANSYS and PFE give $U_x, U_y, \sigma_x, \sigma_y, \tau_{xy}$.

Table 4.10. Displacements at $X = 300\ mm\ and\ Y = -50\ mm$ for Example-2

	U_x	U_y
Beam Theory	0.135000	0.540000
ANSYS Shell Element	0.128740	0.544220
Panel Finite Element	0.130575	0.511142

Table 4.11. Displacements at $X = 300\ mm\ and\ Y = 0\ mm$ for Example-2

	U_x	U_y
Beam Theory	0.0	0.540000
ANSYS Shell Element	0.0	0.540030
Panel Finite Element	0.0	0.506851

Table 4.12. Displacements at $X = 300\ mm\ and\ Y = 50\ mm$ for Example-2

	U_x	U_y
Beam Theory	-0.135000	0.540000
ANSYS Shell Element	-0.129760	0.543800
Panel Finite Element	-0.130575	0.511142

Table 4.13. Stresses at $X = 0\ mm, Y = -50\ mm\ and\ Z = 0\ mm$ for Example-2

	σ_x	σ_s	τ_{xs}
Beam Theory	180.00	0.0	0.0
ANSYS Shell Element	178.74	53.61	10.07
Panel Finite Element	180.00	54.00	1.1

Table 4.14. Stresses at $X = 0\ mm, Y = 0\ mm\ and\ Z = 0\ mm$ for Example-2

	σ_x	σ_s	τ_{xs}
Beam Theory	0.0	0.0	15.00
ANSYS Shell Element	0.0	0.0	9.97
Panel Finite Element	0.0	0.0	12.79

Table 4.15. Stresses at $X = 0\ mm, Y = 50\ mm\ and\ Z = 0\ mm$ for Example-2

	σ_x	σ_s	τ_{xs}
Beam Theory	-180.00	0.0	0.0
ANSYS Shell Element	-178.73	-53.63	9.87
Panel Finite Element	-180.00	-54.00	1.10

Table 4.16. Stresses at $X = 150\ mm, Y = -50\ mm\ and\ Z = 0\ mm$ for Example-2

	σ_x	σ_s	τ_{xs}
Beam Theory	90.00	0.0	0.0
ANSYS Shell Element	89.43	10.92	10.05
Panel Finite Element	90.00	9.83	1.10

Table 4.17. Stresses at $X = 150\ mm, Y = 0\ mm\ and\ Z = 0\ mm$ for Example-2

	σx	σs	τxs
Beam Theory	0.0	0.0	15.00
ANSYS Shell Element	0.0	0.0	9.97
Panel Finite Element	0.0	0.0	12.79

Table 4.18. Stresses at $X = 150\ mm, Y = 50\ mm\ and\ Z = 0\ mm$ for Example-2

	σx	σs	τxs
Beam Theory	-90.00	0.0	0.0
ANSYS Shell Element	-89.45	-10.88	9.89
Panel Finite Element	-90.00	-9.83	1.10

4.3   Example-3

$300 \times 100 \times 2\ mm\ plate, E = 200000\ N/mm^2, v = 0.3$
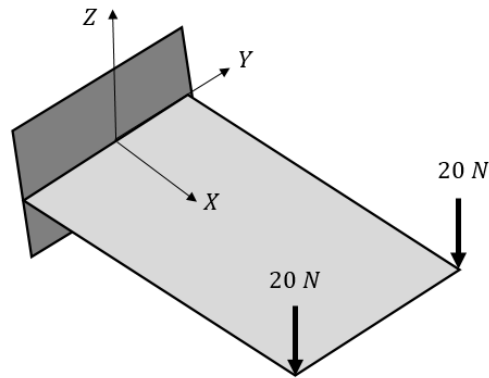

Figure 4.3.Example-3 Graphical Representation

This is an out-of-plane bending problem. In the following, the results obtained by a single PFE are compared with the beam solution and a single ANSYS shell finite element. The beam solution gives U_z and σ_x only. ANSYS and PFE give $U_z, \sigma_x, \sigma_y, \tau_{xy}$.

Table 4.19. Displacements at $X = 300\ mm\ and\ Y = -50\ mm$ for Example-3

	Uz
Beam Theory	-27.000000
ANSYS Shell Element	-24.639000
Panel Finite Element	-24.873884

Table 4.20. Displacements at $X = 300\ mm\ and\ Y = 0\ mm$ for Example-3

	Uz
Beam Theory	-27.000000
ANSYS Shell Element	-24.742000
Panel Finite Element	-24.990764

Table 4.21. Displacements at $X = 300\ mm\ and\ Y = 50\ mm$ for Example-3

	Uz
Beam Theory	-27.000000
ANSYS Shell Element	-24.639000
Panel Finite Element	-24.873884

Table 4.22. Stresses at $X = 0\ mm, Y = -50\ mm\ and\ Z = 1\ mm$ for Example-3

	σx	σs	τxs
Beam Theory	180.00	0.0	0.0
ANSYS Shell Element	178.43	52.01	5.15
Panel Finite Element	180.00	54.00	2.40

Table 4.23. Stresses at $X = 0\ mm, Y = 0\ mm\ and\ Z = 1\ mm$ for Example-3

	σx	σs	τxs
Beam Theory	180.00	0.0	0.0
ANSYS Shell Element	178.43	52.01	0.0
Panel Finite Element	180.00	54.00	0.0

Table 4.24. Stresses at $X = 0\ mm, Y = 50\ mm\ and\ Z = 1\ mm$ for Example-3

	σ_x	σ_s	τ_{xs}
Beam Theory	90.00	0.0	0.0
ANSYS Shell Element	88.96	17.84	1.29
Panel Finite Element	90.00	17.64	2.40

Table 4.25. Stresses at $X = 150\ mm, Y = -50\ mm\ and\ Z = 1\ mm$ for Example-3

	σ_x	σ_s	τ_{xs}
Beam Theory	90.00	0.0	0.0
ANSYS Shell Element	88.96	17.84	1.29
Panel Finite Element	90.00	17.65	2.40

Table 4.26. Stresses at $X = 150\ mm, Y = 0\ mm\ and\ Z = 1\ mm$ for Example-3

	σ_x	σ_s	τ_{xs}
Beam Theory	90.00	0.0	0.0
ANSYS Shell Element	88.96	17.84	0.0
Panel Finite Element	90.00	17.65	0.0

Table 4.27. Stresses at $X = 150\ mm, Y = 50\ mm\ and\ Z = 1\ mm$ for Example-3

	σ_x	σ_s	τ_{xs}
Beam Theory	90.00	0.0	0.0
ANSYS Shell Element	88.96	17.84	-1.29
Panel Finite Element	90.00	17.65	-2.40

4.4   Example-4

$300 \times 100 \times 2 \ mm \ plate, E = 200000 \ N/mm^2, v = 0.3$
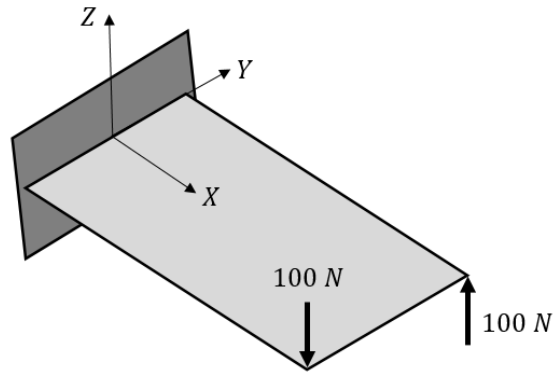

Figure 4.4. Example-4 Graphical Representation

This is a torsion problem. In the following, the results obtained by a single PFE are compared with the beam solution and a single ANSYS shell finite element. The beam solution gives U_z and τ_{xy} only. ANSYS and PFE give $U_z, \sigma_x, \sigma_y, \tau_{xy}$.

Table 4.28. Displacements at $X = 300 \ mm \ and \ Y = -50 \ mm$ for Example-4

	U_z
Beam Theory	-6.327592
ANSYS Shell Element	-6.752600
Panel Finite Element	-6.318812

Table 4.29. Displacements at $X = 300 \ mm \ and \ Y = 0 \ mm$ for Example-4

	U_z
Beam Theory	0.0
ANSYS Shell Element	0.0
Panel Finite Element	0.0

4.30. Displacements at $X = 300\ mm$ and $Y = 50\ mm$ for Example-4

	U_z
Beam Theory	6.327592
ANSYS Shell Element	6.752600
Panel Finite Element	6.318812

Table 4.31. Stresses at $X = 150\ mm$, $Y = -50\ mm$ and $Z = 1\ mm$ for Example-4

	σ_x	σ_s	τ_{xs}
Beam Theory	0.0	0.0	-74.79
ANSYS Shell Element	5.41	7.44	-67.23
Panel Finite Element	13.49	4.05	-83.05

Table 4.32. Stresses at $X = 150\ mm$, $Y = 0\ mm$ and $Z = 1\ mm$ for Example-4

	σ_x	σ_s	τ_{xs}
Beam Theory	0.0	0.0	-74.79
ANSYS Shell Element	0.0	0.65	-69.20
Panel Finite Element	0.0	0.0	-83.05

Table 4.33. Stresses at $X = 150\ mm$, $Y = 50\ mm$ and $Z = 1\ mm$ for Example-4

	σ_x	σ_s	τ_{xs}
Beam Theory	0.0	0.0	-74.79
ANSYS Shell Element	-5.38	-6.14	-71.17
Panel Finite Element	-13.49	-4.05	-83.05

4.5   Example-5

$300 \times 100 \times 2\ mm\ plate, E = 200000\ N/mm^2, v = 0.3$
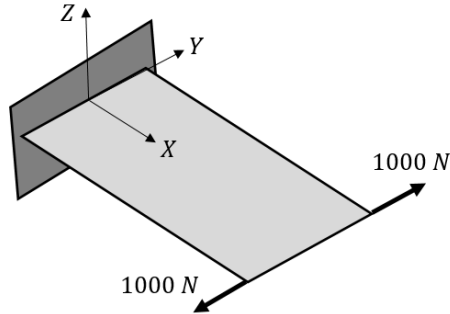
Figure 4.5. Example-5 Graphical Representation

This is a distortion problem which cannot be solved by beam theories since the net loading on the beam is zero. In the following, the results obtained by a single PFE and a single ANSYS shell finite element are compared.

Table 4.34. Displacements at $X = 300\ mm\ and\ Y = -50\ mm$ for Example-5

	U_x	U_y
ANSYS Shell Element	-0.000881	-0.007299
Panel Finite Element	-0.007168	-0.004801

Table 4.35. Displacements at $X = 300\ mm\ and\ Y = 0\ mm$ for Example-5

	U_x	U_y
ANSYS Shell Element	0.000304	0.0
Panel Finite Element	-0.006270	0.0

Table 4.36. Displacements at $X = 300\ mm\ and\ Y = 50\ mm$ for Example-5

	U_x	U_y
ANSYS Shell Element	-0.000881	0.004801
Panel Finite Element	-0.007168	0.007299

Table 4.37. Stresses at $X = 300\ mm, Y = -50\ mm\ and\ Z = 0\ mm$ for Example-5

	σ_x	σ_s	τ_{xs}
ANSYS Shell Element	0.0	9.80	1.19
Panel Finite Element	4.37	30.51	0.89

Table 4.38. Stresses at $X = 300\ mm, Y = 0\ mm\ and\ Z = 0\ mm$ for Example-5

	σ_x	σ_s	τ_{xs}
ANSYS Shell Element	0.0	9.80	0.0
Panel Finite Element	5.03	30.71	0.0

Table 4.39. Stresses at $X = 300\ mm, Y = 50\ mm\ and\ Z = 0\ mm$ for Example-5

	σ_x	σ_s	τ_{xs}
ANSYS Shell Element	0.0	9.80	-1.19
Panel Finite Element	4.37	30.51	-0.89

4.6   Example-6

An L-beam is subjected to a torque which creates twisting and a transverse force which creates bending in two planes.

L-beam: $100 \times 50\ mm, t = 2\ mm, E = 200000, \nu = 0.3$.
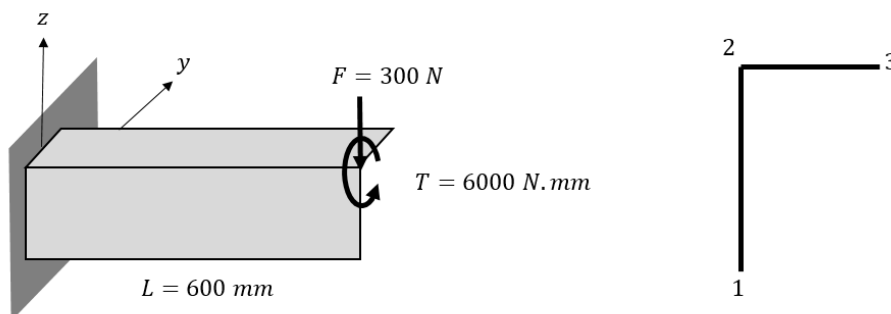
Figure 4.6. Example-6 Graphical Representation

The displacement and stress results obtained by using the PFE are compared with the beam theory and the ANSYS shell finite element modelling. In this example, a convergence analysis for the ANSYS solutions is performed in order to decide on the optimum element size to be used in the ANSYS shell models in this and the forthcoming examples.

The convergence study is performed using meshes with element sizes of 50x50, 25x25, 16.67x16.67, 12.5x12.5 and 10x10 mm. The displacement and normal stress magnitudes are as follows in Table 4.40.

Table 4.40. Displacement Results for Cantilever L-Beam

# of Elements	Element size (mm x mm)	U_z ($X = 300\ mm$, $Y = -8.33\ mm$, $Z = 33.33\ mm$)	σ_x ($X = 0\ mm$, $Y = -8.33\ mm$, $Z = 33.33\ mm$)
36	50x50	-0.155640	33.86
144	25x25	-0.156640	36.02
324	16.67x16.67	-0.156940	37.62
564	12.5x12.5	-0.157110	38.98
868	10x10	-0.157130	39.10

The displacement and stress results converged as the mesh density increased. In order to select an optimum element size, we prepared a percentage change table and obtain a percentage change which is less than 1%, which is 10 mm x 10 mm, as shown in Table 4.41.

Table 4.41. Shell Modelling Convergence Analysis (Percentage Changes)

Number, n	Element size (mm x mm)	ΔU_z %	$\Delta \sigma_x$ %
1	50x50	-	-
2	25x25	0.64	6.38
3	16.67x16.67	0.19	4.45
4	12.5x12.5	0.11	3.61
5	10x10	0.01	0.31

Also, the displacement (U_z) and stress (σ_x) results are tabulated as graphs in order to show the mesh convergence, as shown below:
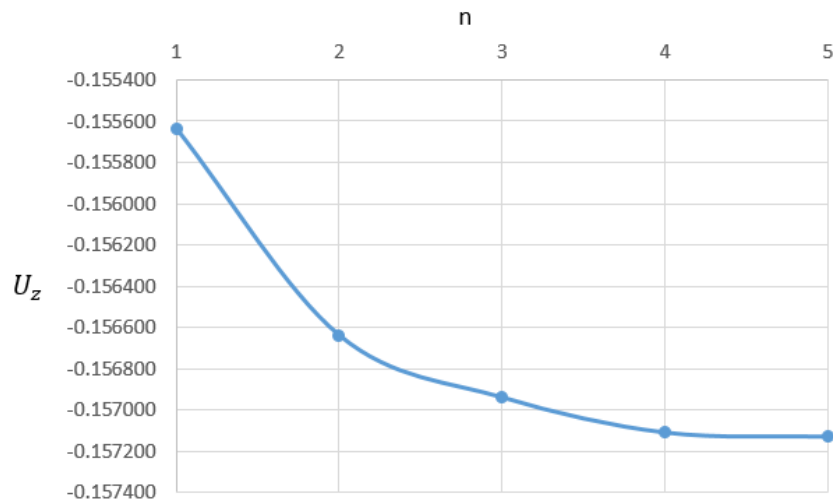
Figure 4.7. Displacement (U_z) plot for shell mesh convergence analysis
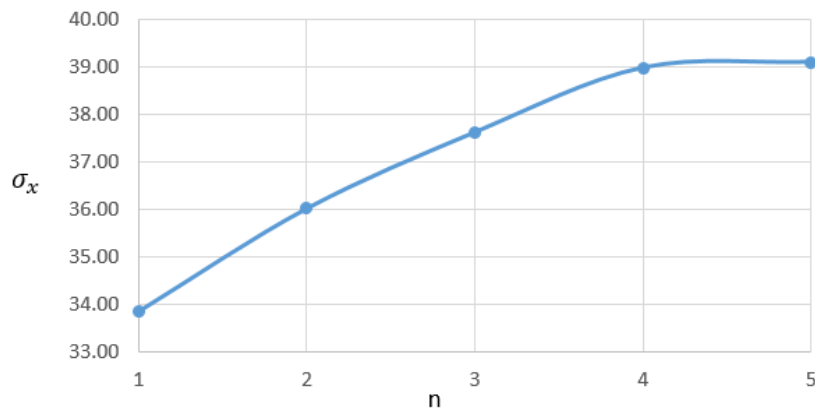
Figure 4.8. Stress (σ_x) plot for shell mesh convergence analysis

Therefore, in the Examples 6-9, a square shell element of size 10 mm x 10 mm is used in the shell models. As an exception, in the Example-7 where the half length of the flanges in the I-section is 25 mm, the shell element size will be 5 mm x 5 mm.

The numbers of elements and degrees of freedom of the shell model and PFE are tabulated below for comparison:

Table 4.42. No. of Elements and DOFs for Example-6

	Number of Elements	Number of DOFs
ANSYS Shell	868	5550
PFE	6	105

The 3D deformation shapes with total displacement color graphics, the displacements and the stress results are given in the next figures for Example-6.
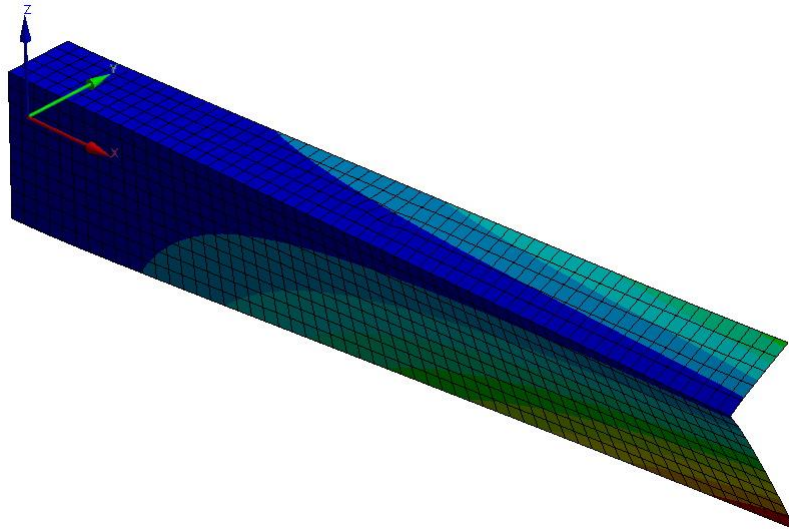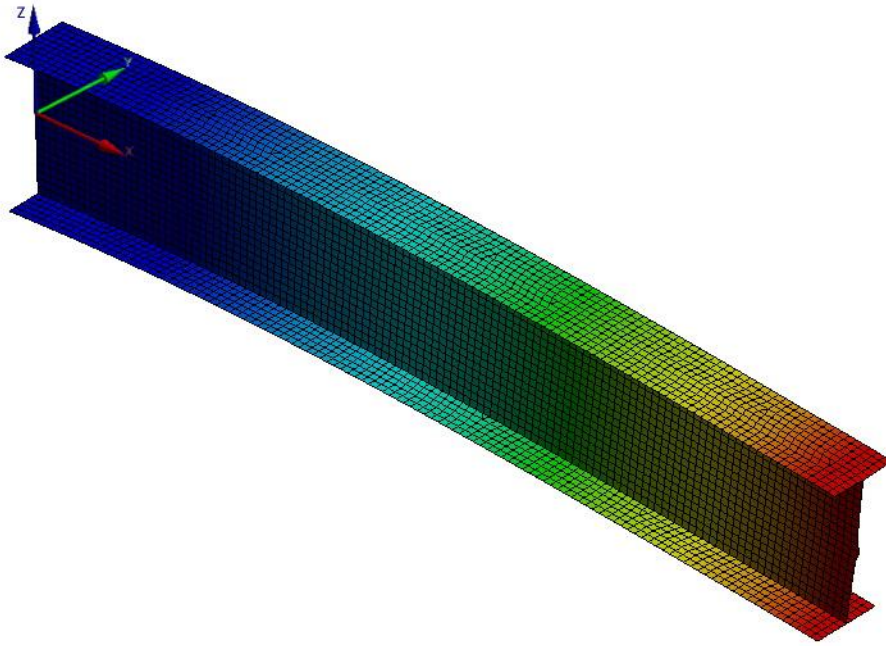

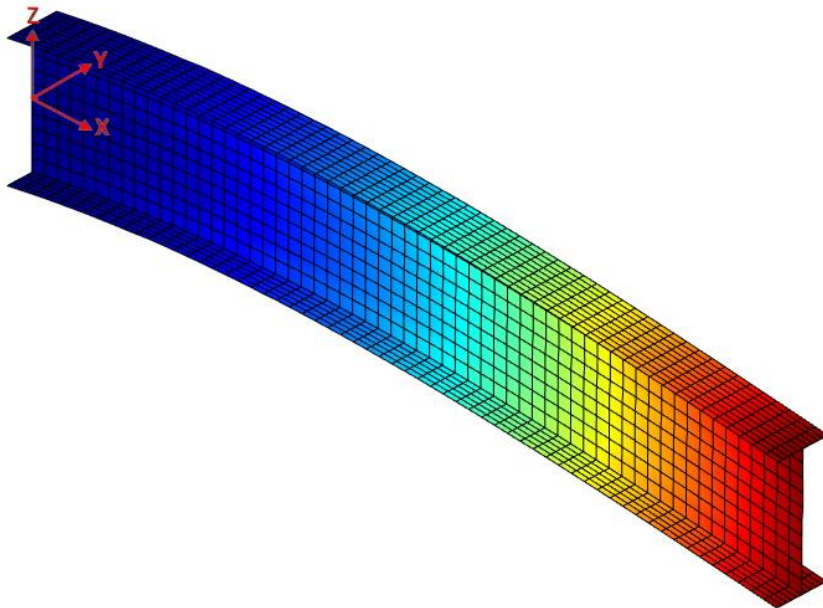Figure 4.9. ANSYS shell deformation shape for Example-6
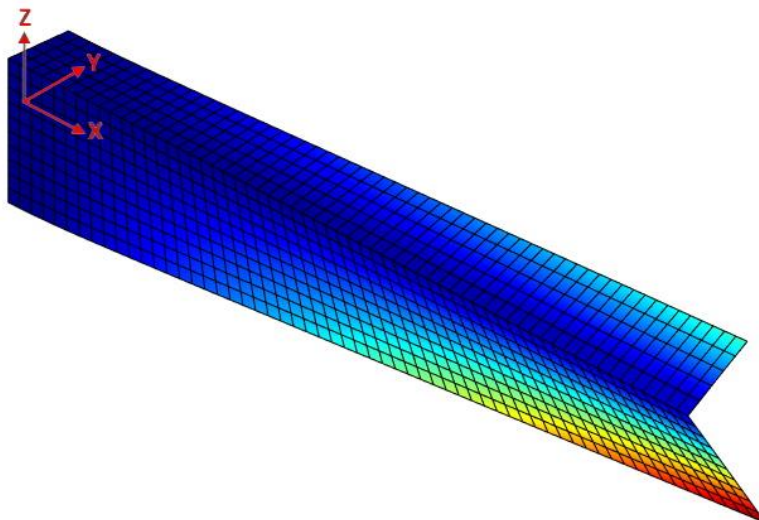
Figure 4.10. Panel finite element method deformation shape for Example-6
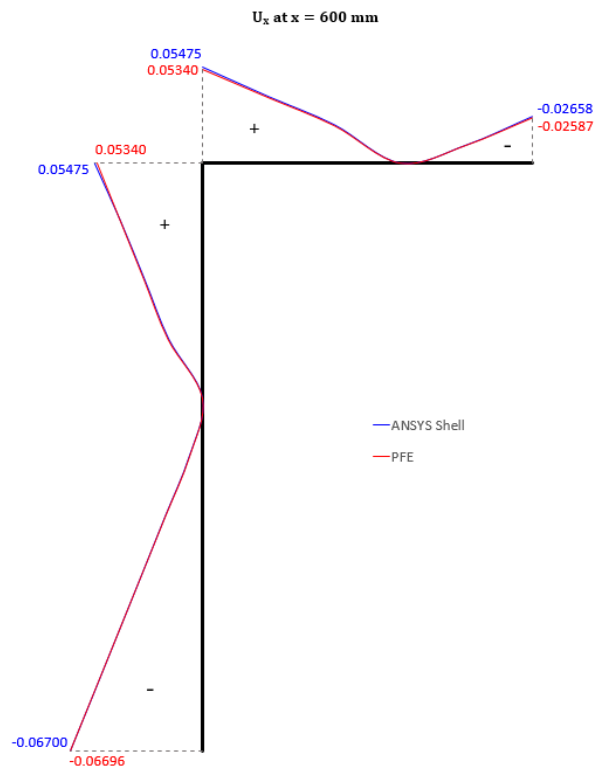
Figure 4.11. Comparison of U_x displacements for Example-6
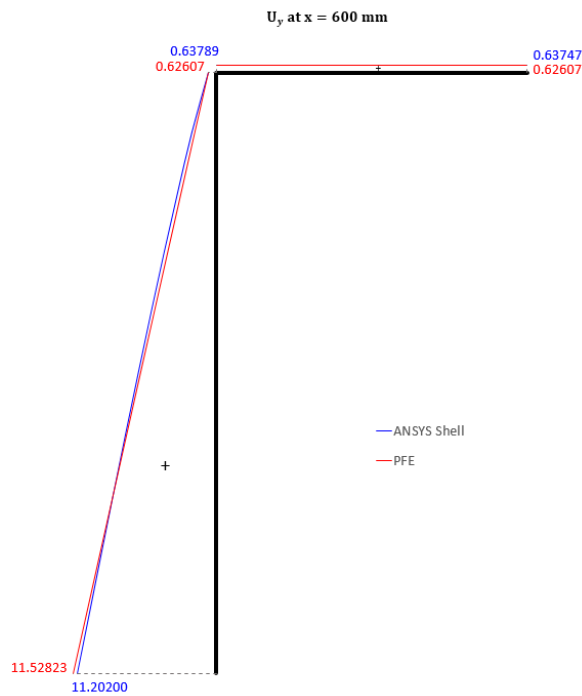
Figure 4.12. Comparison of U_y displacements for Example-6
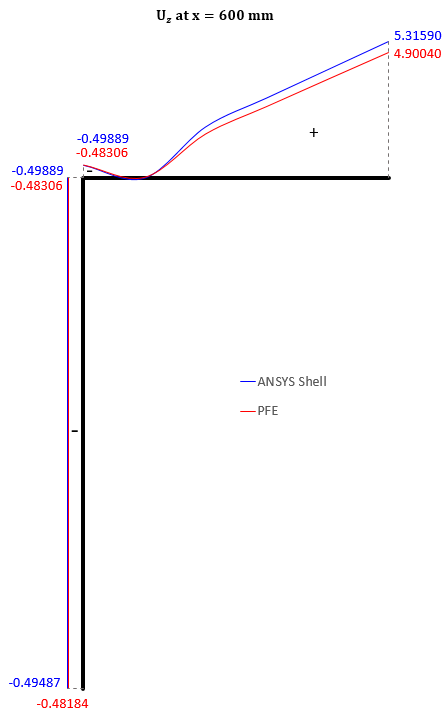
Figure 4.13. Comparison of U_z displacements for Example-6
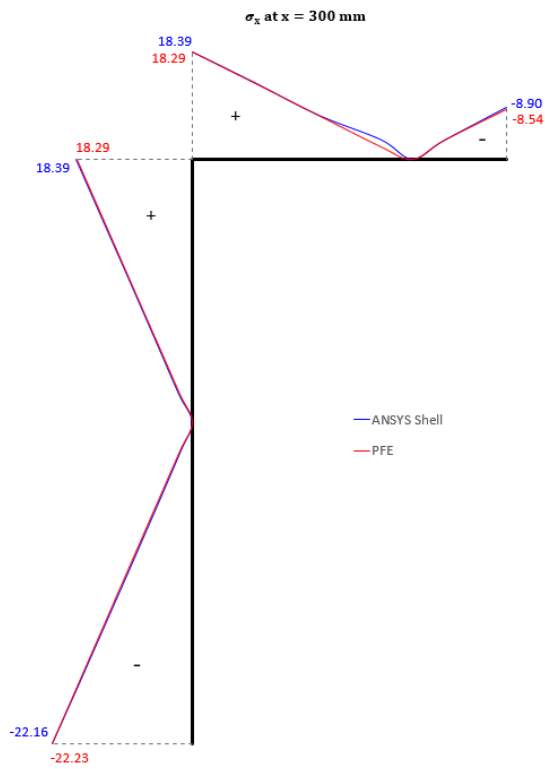
Figure 4.14. Comparison of σ_x normal stresses for Example-6
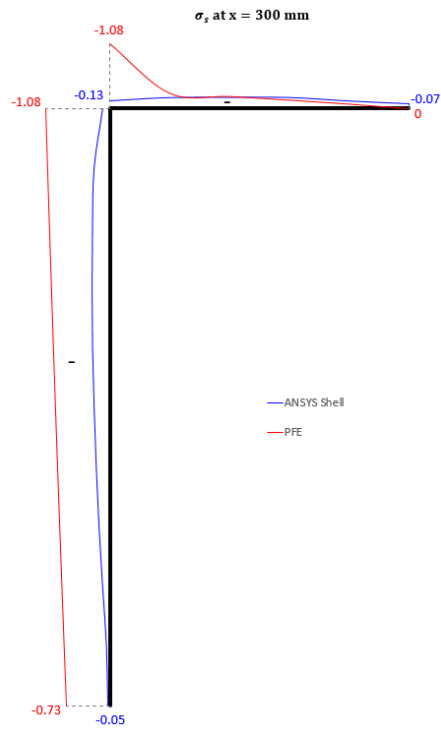
Figure 4.15. Comparison of σ_s normal stresses for Example-6
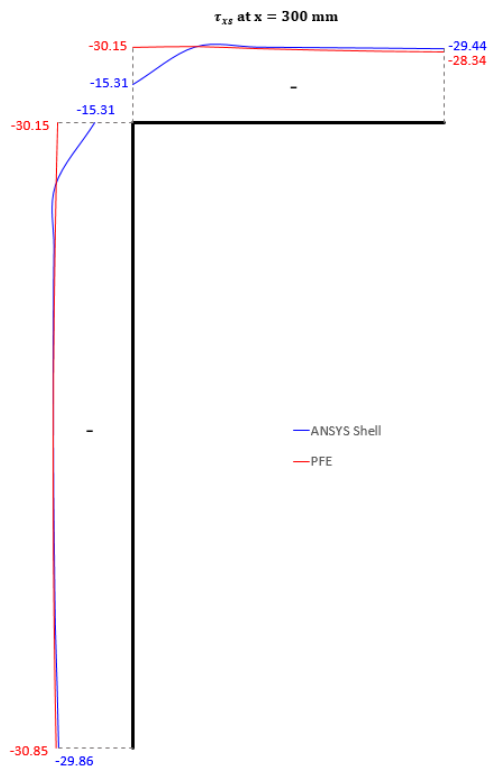
Figure 4.16. Comparison of τ_{xs} shear stresses for Example-6

4.7   Example-7

The bending of an I-beam is analyzed considering the effect of stress stiffening caused by the axial force.

I-beam: $50 \times 100 \times 50 \ mm, t = 2 \ mm, E = 200000, v = 0.3$.
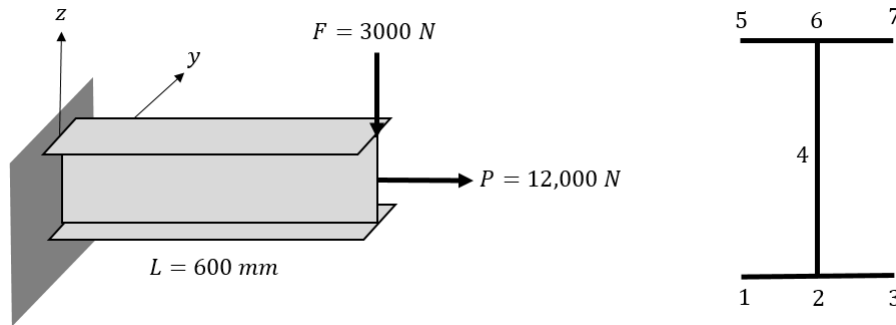
Figure 4.17. Example-7 Graphical Representation

The numbers of elements and degrees of freedom of the shell model and PFE are tabulated below for comparison:

Table 4.43. No. of Elements and DOFs for Example-7

	Number of Elements	**Number of DOFs**
ANSYS Shell	4718	28950
PFE	6	105

The displacement and stress results obtained by using the PFE are compared with the beam theory and the ANSYS shell finite element modelling. The 3D deformation shapes with total displacement color graphics, the displacements and the stress results are given in the next figures for Example-7.

Figure 4.18. ANSYS shell deformation shape for Example-7

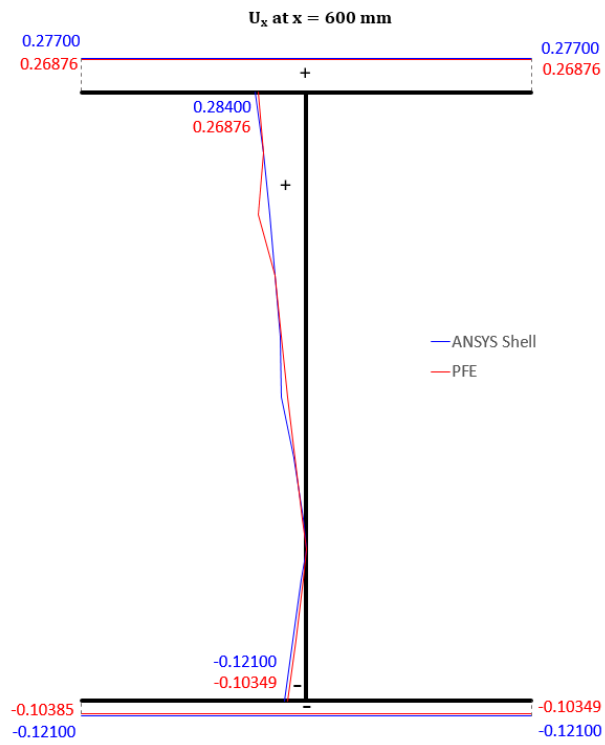Figure 4.19. Panel finite element method deformation shape for Example-7

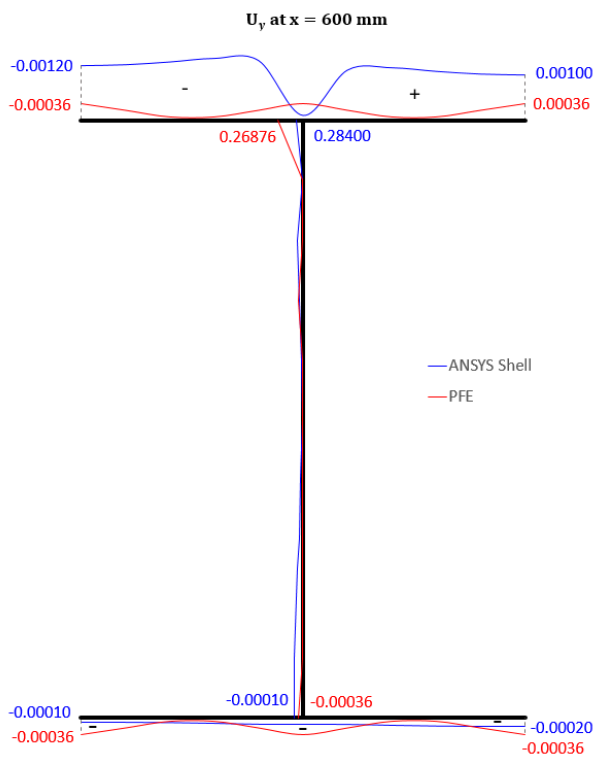Figure 4.20. Comparison of U_x displacements for Example-7

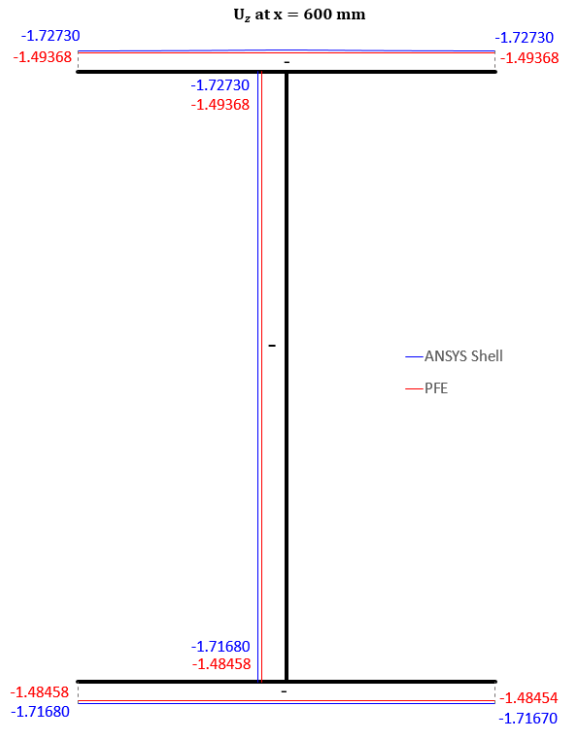Figure 4.21. Comparison of U_y displacements for Example-7

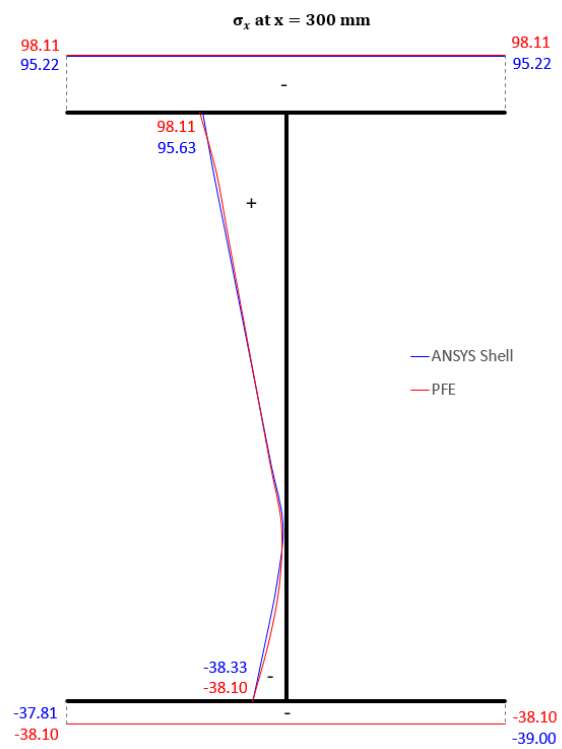Figure 4.22. Comparison of U_z displacements for Example-7

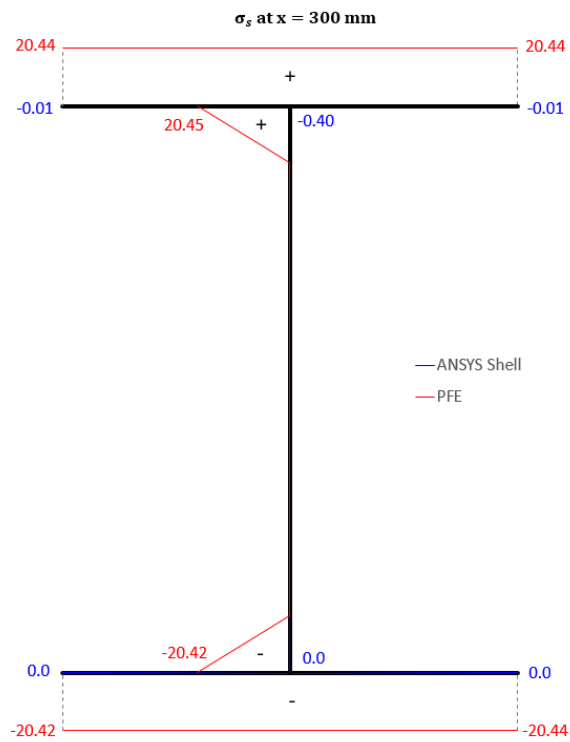Figure 4.23. Comparison of σ_x normal stresses for Example-7

Figure 4.24. Comparison of σ_s normal stresses for Example-7
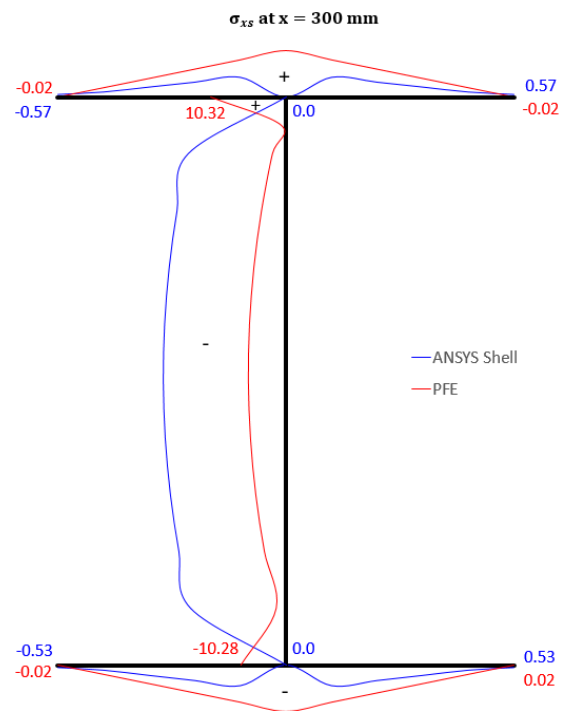

Figure 4.25. Comparison of τ_{xs} shear stresses for Example-7

47

4.8   Example-8

The U-beam is subjected to distributed transverse force which bending and torsion. The axial force creates extension, bending, twisting and warping. The stress stiffening effect of the axial force is included.

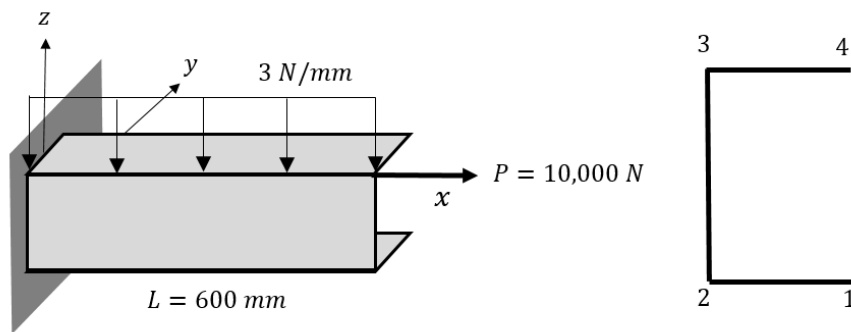U-beam: $50 \times 100 \times 50 \ mm, t = 2 \ mm, E = 200000, v = 0.3$.

Figure 4.26. Example-8 Graphical Representation

The numbers of elements and degrees of freedom of the shell model and PFE are tabulated below for comparison:

Table 4.44. No. of Elements and DOFs for Example-8

	Number of Elements	Number of DOFs
ANSYS Shell	1156	7272
PFE	6	105

The displacement and stress results obtained by using the PFE are compared with the beam theory and the ANSYS shell finite element modelling. The 3D deformation shapes with total displacement color graphics, the displacements and the stress results are given in the next figures for Example-8.
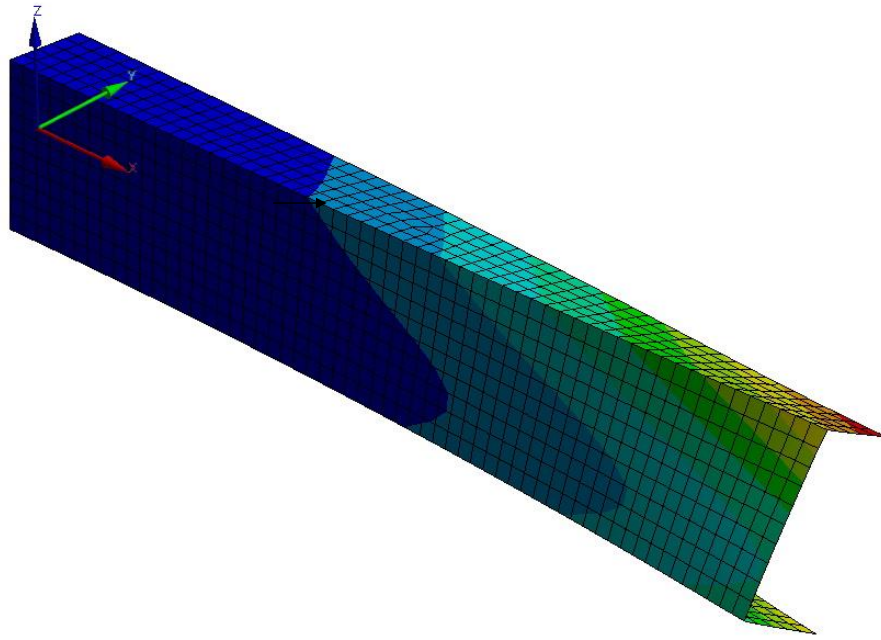
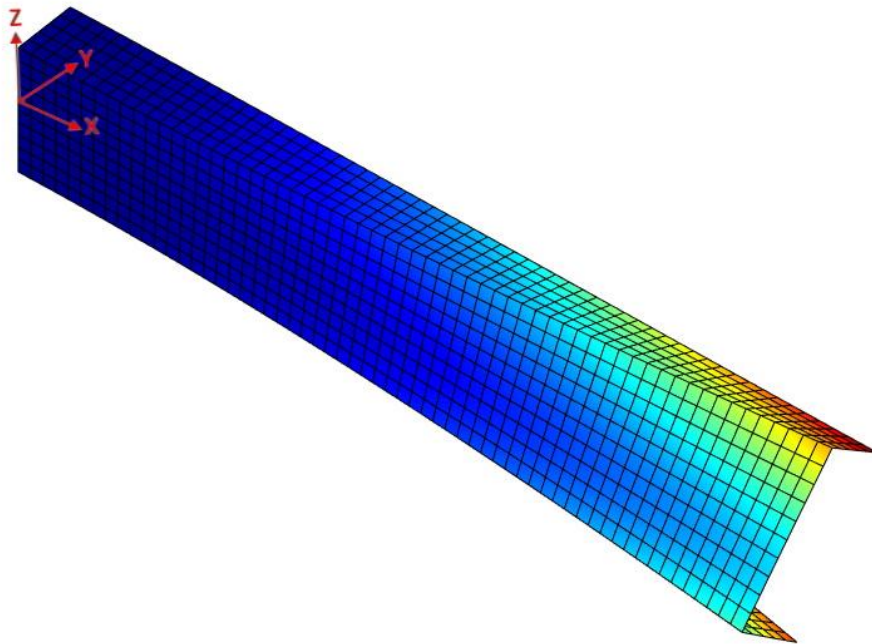Figure 4.27. ANSYS shell deformation shape for Example-8

Figure 4.28. Panel finite element method deformation shape for Example-8
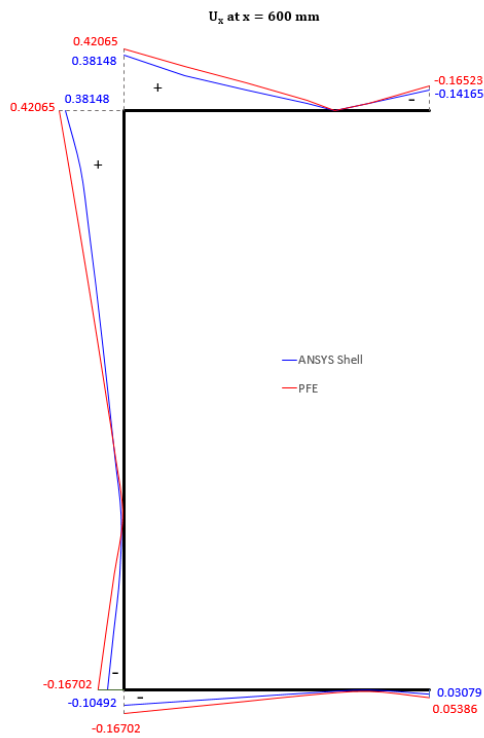
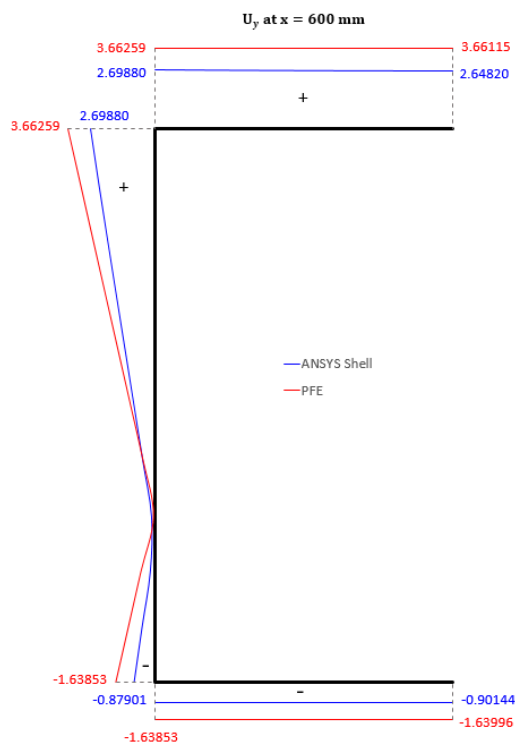Figure 4.29. Comparison of U_x displacements for Example-8

Figure 4.30. Comparison of U_y displacements for Example-8

Figure 4.31. Comparison of U_z displacements for Example-8
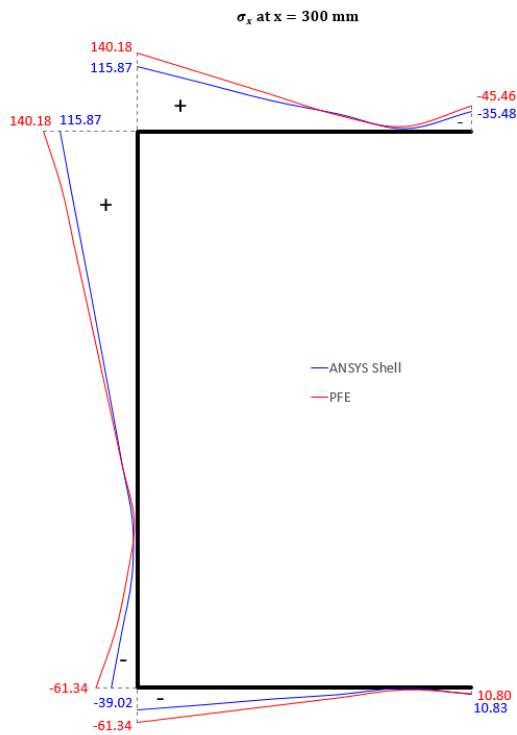
Figure 4.32. Comparison of σ_x normal stresses for Example-8

51

Figure 4.33. Comparison of σ_s normal stresses for Example-8
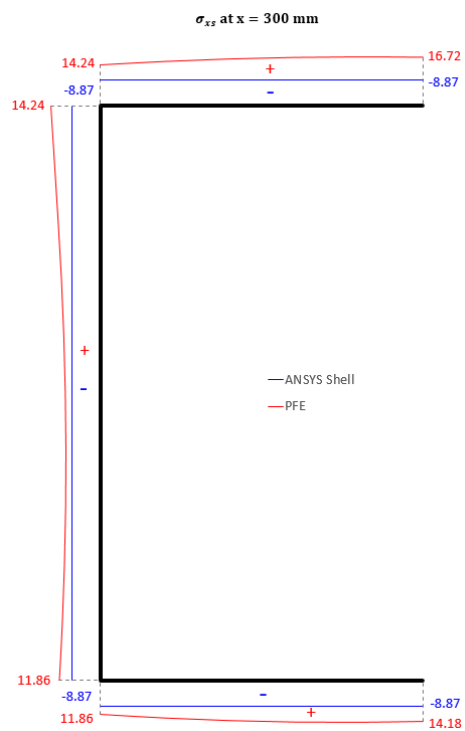
Figure 4.34. Comparison of τ_{xs} shear stresses for Example-8

52

4.9   Example-9

A Z-beam is subjected to a transverse force which creates bending in two planes and an axial force which creates twisting and warping. The effect of stress stiffening due to axial force is included.

Z-beam: $50 \times 100 \times 50 \, mm$, $t = 2 \, mm$, $E = 200000$, $v = 0.3$.
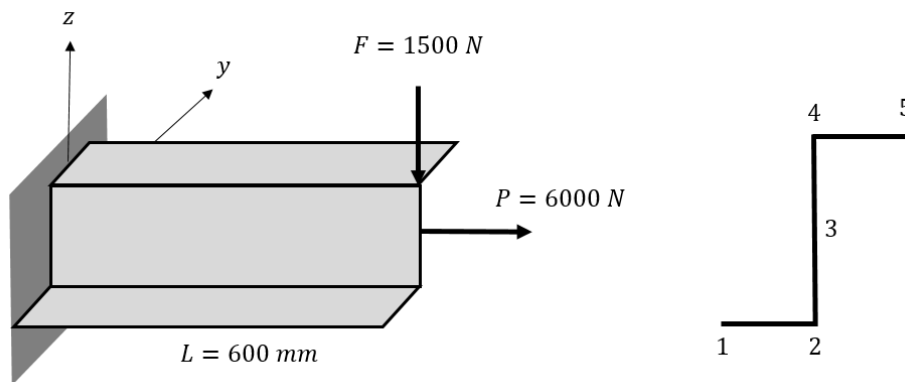
Figure 4.35. Example-9 Graphical Representation

The numbers of elements and degrees of freedom of the shell model and PFE are tabulated below for comparison:

Table 4.45. No. of Elements and DOFs for Example-9

	Number of Elements	Number of DOFs
ANSYS Shell	1190	7488
PFE	6	105

The displacement and stress results obtained by using the PFE are compared with the beam theory and the ANSYS shell finite element modelling. The 3D deformation shapes with total displacement color graphics, the displacements and the stress results are given in the next figures for Example-9.
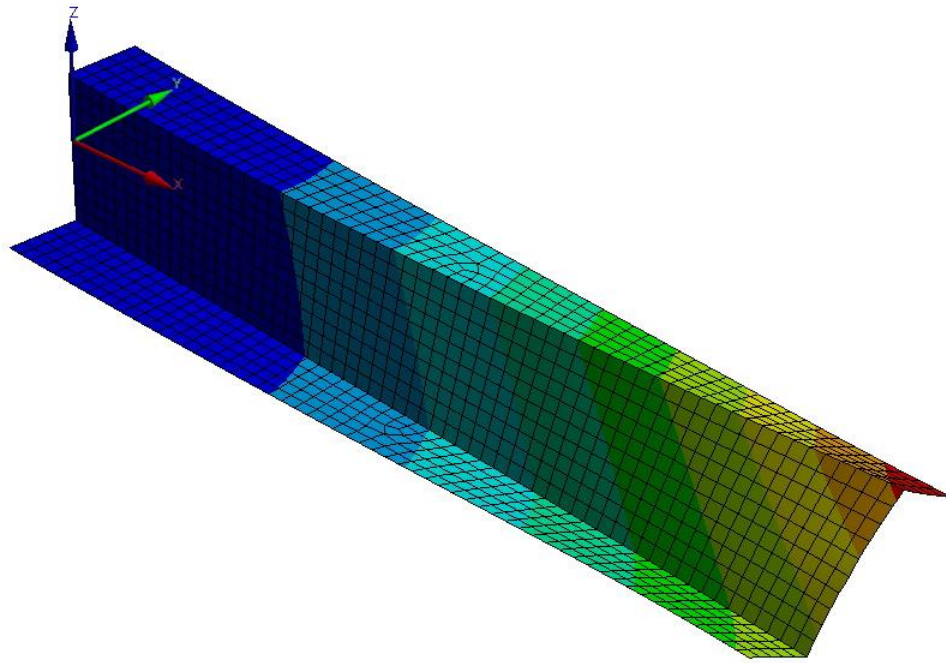
Figure 4.36. ANSYS shell deformation shape for Example-9
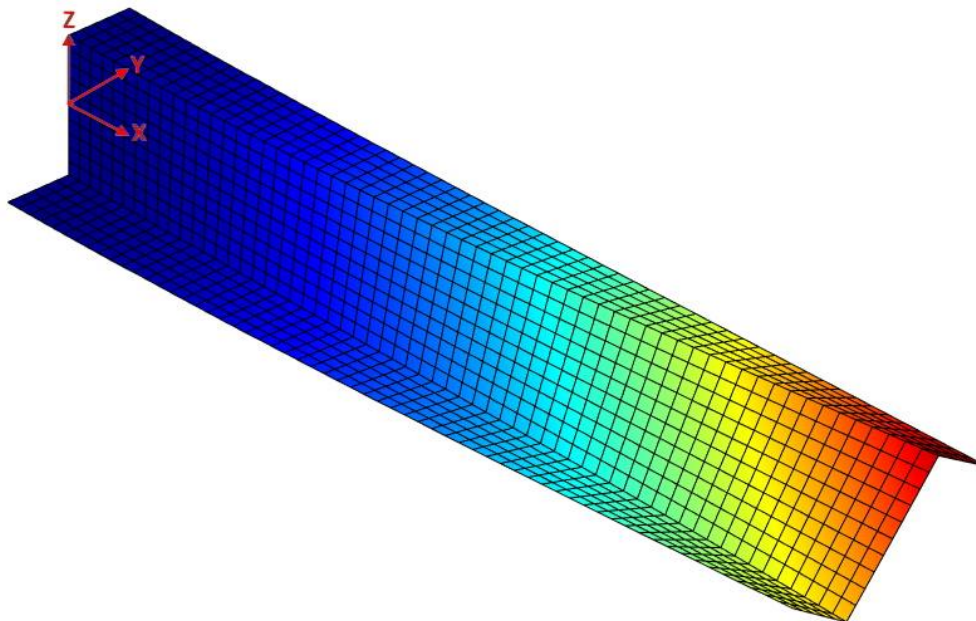
Figure 4.37. Panel finite element method deformation shape for Example-9

Figure 4.38. Comparison of U_x displacements for Example-9

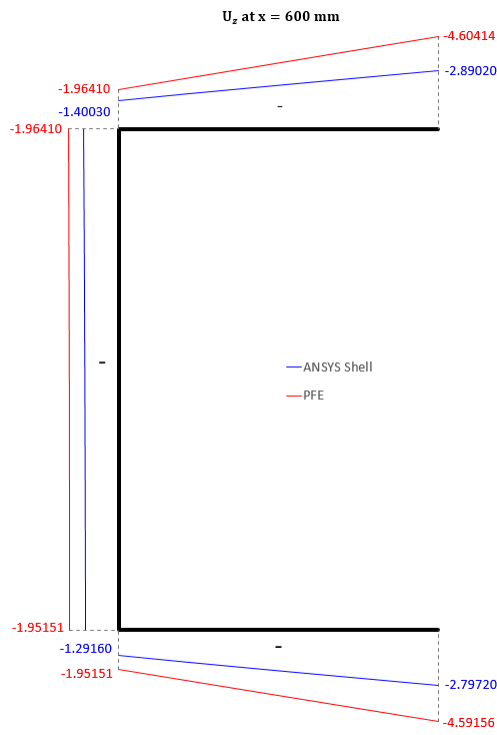Figure 4.39. Comparison of U_y displacements for Example-9

Figure 4.40. Comparison of U_z displacements for Example-9

Figure 4.41. Comparison of σ_x normal stresses for Example-9

56

Figure 4.42. Comparison of σ_s normal stresses for Example-9

Figure 4.43. Comparison of τ_{xs} normal stresses for Example-9

CHAPTER 5

CONCLUSIONS

In this thesis, a finite element for the analysis of open section thin walled beams has been developed. In this formulation, rigid and in-plane and out-of-plane elastic motions of the cross section are cons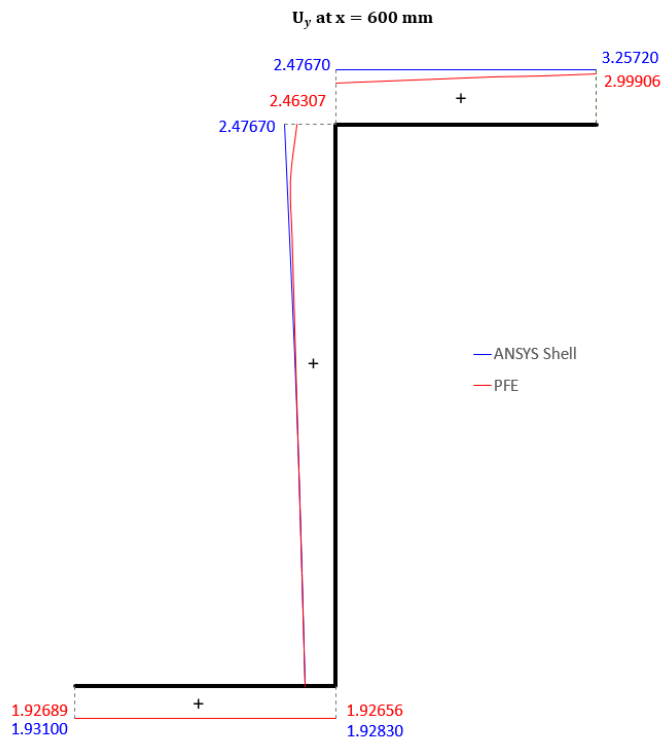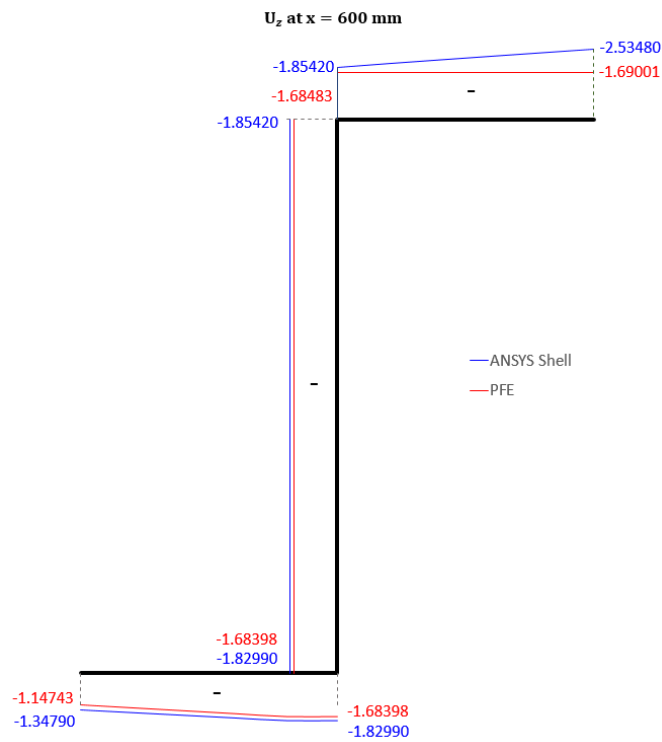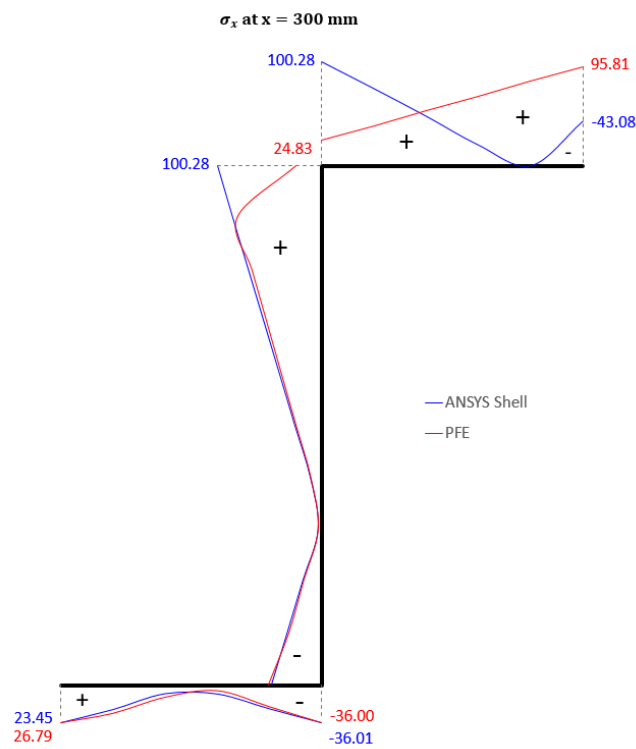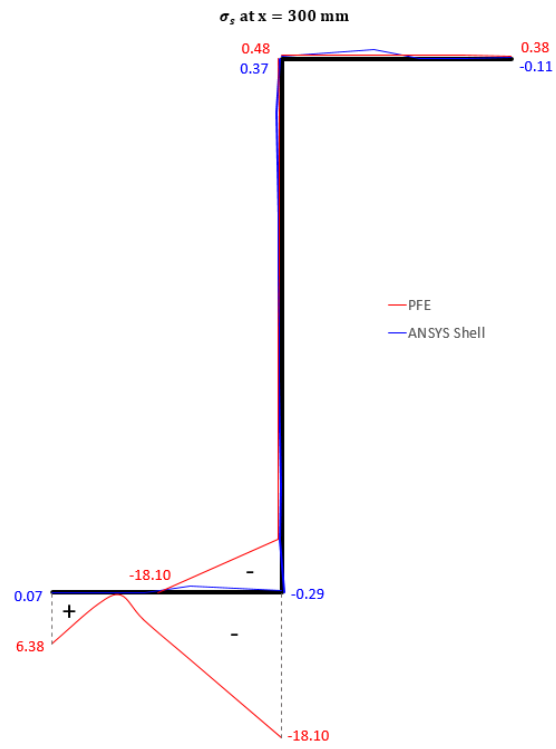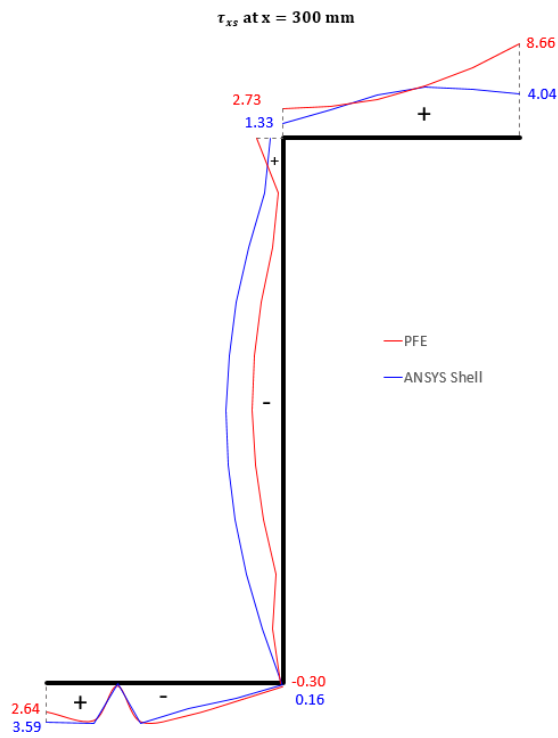idered by adding elastic modes of deformation to the Vlasov displacement field assumption. The displacement components are assumed by linear or quadratic polynomials. The beam finite element is the assembly of panel finite elements and the number of element degrees of freedom is independent of the number of panels. The stress stiffening due to axial loads is also taken into account. The accuracy of the present method is higher than that of Vlasov finite element and is lower than that of shell finite elements as expected. The computational cost of the present formulation is incomparably lower than a shell analysis. Hence the objective of this thesis has been fulfilled.

The majority of the studies in this field are based on superposing natural modes of the beam cross section to assume displacements (NMM). In the present study (PFE), this approach has not been used due to following reasons:

i)   NMM requires solution of an eigenvalue problem to determine the natural modes of the cross section. If the cross section is nonuniform, then a number of eigenvalue analyses are necessary for each different cross section in the beam. In PFE, there is no need for eigenvalue analysis and nonuniformity does not present any difficulty since each finite element may be composed of different number of panels having different geometries.

ii)　The selection of natural modes in NMM is not straightforward. If the beam geometry and loading are simple, then a few lowest natural modes are sufficient to assume the displacement field. However, in more complicated cases, higher modes are necessary and it is difficult to choose the right ones.

iii)　In NMM, the number of element degrees of freedom is dependent on the number of natural modes considered. This causes a difficulty in programming. In PFE, the number of element degrees of freedom is 30 and is independent of the number of panels.

The present method can be extended to the analysis of closed section thin walled beams, dynamic analysis under transient loadings, advanced material beams and problems with material and geometric nonlinearities.

REFERENCES

[1]   V.Z. Vlasov, "Thin-Walled Elastic Bars" (in Russian), 2nd ed., *Fizmatgiz*, Moscow, 1959.

[2]   M. Capurso, "Sul calcolo dei sistemi spaziali di controventamento", *Giornale del Genio Civile*, 1–2–3, (1981), 27–42 (in Italian).

[3]   Schardt R. "Eine Erweiterung der Technischen Biegetheorie zur Berechnung prismatischer Faltwerke". *Der Stahlbau* 1966;35:161–71.

[4]   Schardt R. "Anwendung der Erweiterten Technischen Biegetheorie auf die Berechnung prismatischer Faltwerke und Zylinderschalen nach Theorie I. und II. Ordnung". *Proceedings of the IASS-Symposium on Folded Plates and Prismatic Structures*, Wien, vol. I. 1970.

[5]   Schardt R. "Generalized beam theory—an adequate method for coupled stability problems". *ThinWalled Structures*, 1994;19:161–80

[6]   Andreassen, M.J., 2012. "Distortional Mechanics of Thin-Walled Structural Elements". *Thesis (PhD)*. Department of Civil Engineering, Technical University of Denmark.

[7]   Jeppe Jönsson, "Distortional theory of thin-walled beams", *Thin-Walled Structures*, Volume 33, Issue 4, 1999, Pages 269-303.

[8]   Anders Bau Hansen, Jeppe Jönsson, "Displacement modes of a thin-walled beam model with deformable cross sections", *Thin-Walled Structures*, Volume 141, 2019, Pages 576-592

[9]   Zhang, L.; Zhu, W.; Ji, A.; Peng, L. "A Simplified Approach to Identify Sectional Deformation Modes of Thin-Walled Beams with Prismatic Cross-Sections". *Appl. Sci.* 2018, 8, 1847.

[10] Zhang, L.; Ji, A.; Zhu, W. "A Novel Approach to Perform the Identification of Cross-Section Deformation Modes for Thin-Walled Structures in the Framework of a Higher Order Beam Theory". *Appl. Sci.* 2019, 9, 5186.

[11] Ghose, D., 1991. "Finite Element Formulation of a Thin-Walled Beam with Improved Response to Warping Restraint". *Thesis (MS)*. Department of Aerospace & Ocean Engineering, Virginia Polytechnic Institute and State University.

[12] Wen Yi Lin, Kuo Mo Hsiao, "More general expression for the torsional warping of a thin-walled open-section beam", *International Journal of Mechanical Sciences*, Volume 45, Issue 5, 2003, Pages 831-849.

[13] Seok Heo, Jin Hong Kim, Yoon Young Kim, "Significance of distortion in thin-walled closed beam section design", *International Journal of Solids and Structures*, Volume 40, Issue 3, 2003, Pages 633-648.

[14] E.J. Sapountzakis, V.G. Mokos, "Dynamic analysis of 3-D beam elements including warping and shear deformation effects", *International Journal of Solids and Structures*, Volume 43, Issues 22–23, 2006, Pages 6707-6726.

[15] J. Murín, V. Kutiš, "An effective finite element for torsion of constant cross-sections including warping with secondary torsion moment deformation effect", *Engineering Structures*, Volume 30, Issue 10, 2008, Pages 2716-2723.

[16] Li, Haifeng & Luo, Y.. (2010). "Application of stiffness matrix of a beam element considering section distortion effect". *Journal of Southeast University* (English Edition). 26. 431-435.

[17] Mohammed Khalil Ferradi, Xavier Cespedes, Mathieu Arquier, "A higher order beam finite element with warping eigenmodes", *Engineering Structures*, Volume 46, 2013, Pages 748-762.

[18] Alessandra Genoese, Andrea Genoese, Antonio Bilotta, Giovanni Garcea, "A generalized model for heterogeneous and anisotropic beams including section distortions", *Thin-Walled Structures*, Volume 74, 2014, Pages 85-103.

[19] R.F. Vieira, F.B. Virtuoso, E.B.R. Pereira, "A higher order model for thin-walled structures with deformable cross-sections", *International Journal of Solids and Structures*, Volume 51, Issues 3–4, 2014, Pages 575-598.

[20] Sasa Gao. "Development of a new 3D beam finite element with deformable section". *Thesis (PhD)*. Université de Lyon, 2017.

[21] Giovanni Garcea, Rodrigo Gonçalves, Antonio Bilotta, David Manta, Rui Bebiano, Leonardo Leonetti, Domenico Magisano, Dinar Camotim, "Deformation modes of thin-walled members: A comparison between the method of Generalized Eigenvectors and Generalized Beam Theory", *Thin-Walled Structures*, Volume 100, 2016, Pages 192-212.

[22] Latalski, J and Zulli, D. "Generalized Beam Theory for Thin-Walled Beams with Curvilinear Open Cross-Sections". *Applied Sciences*. 2020; 10(21):7802.

[23] Jaeyong Kim, Soomin Choi, Yoon Young Kim, Gang-Won Jang, "Hierarchical derivation of orthogonal cross-section modes for thin-walled beams with arbitrary sections", *Thin-Walled Structures*, Volume 161, 2021, 107491.

CURRICULUM VITAE

PERSONAL INFORMATION

Name and Surname :   Suat Ontaç

Nationality   :

Date of Birth   :

Place of Birth   :

Phone   :

E-mail   :

EDUCATION

Degree	Institution	Year of Graduation
MS	METU Mechanical Engineering	2008
BS	METU Mechanical Engineering	2005
Vocational School	METU Industrial Automation	1999
High School	Çanakkale High School	1993

WORK EXPERIENCE

Year	Company/Institution	Role
2005-Present	TÜBİTAK Uzay Teknolojileri Araştırma Enstitüsü	Group Leader
2005	Başarı Elektronik	Design
2000-2003	Havelsan	Mechanical

FOREIGN LANGUAGES

Advanced English

PUBLICATIONS

1. Ontaç S., Aydın B.Ç., Çetin M., Yurttaş Y., Akın M, Akın B. "Design, Analysis and Manufacture of Composite Overwrapped Xenon Propellant Tank", 35th International Electric Propulsion Conference, IEPC 2017 (2017)

2. Ontaç S. et al. "Innovative Thermal management Concepts for Sharp Leading Edges of Hypersonic Vehicles", Materials Science & Technology Conference 2014 (2014)

3. Ontaç S. et al. "Overview of TUBITAK UZAY's Electric Propulsion Development Project (HALE)", 6th International Conference on Recent Advances in Space Technologies, RAST 2013 (2013)

4. Ontaç S. "Stress Analysis of the RASAT Satellite Structure Considering Vibration Induced Loads during Launch", 3rd CEAS Air & Space Conference, CEAS 2011 (2011)

5. Ontaç S., Ertürk C.L., Soysal S., Çetin M., Nasuhoğlu R.N. "Evaluation and Comparison of Finite Element Dynamic Analyses and Vibration Test Results of Structural Model of RASAT Satellite", 5nd International Conference on Recent Advances in Space Technologies, RAST 2011 (2011)

6. Ontaç. S., Dağ S., Gökler M.İ. "Structural Finite Element Analysis of Stiffened and Honeycomb Panels of the RASAT Satellite", 3nd International Conference on Recent Advances in Space Technologies, RAST 2007 (2007)

7. Ontaç S. "Mechanical Design and Analysis of Small Satellite Structures", The 12th International Conference on Machine Design and Production, UMTİK 2006 (2006)